

# Temperature changes reveal different transcriptional responses in the larvae of the bark beetle *Dendroctonus rhizophagus* during the cold season

Received: 2 April 2025

Accepted: 16 February 2026

Published online: 24 February 2026

Cite this article as: Becerril M., Zúñiga G., Torres-Banda V. *et al.* Temperature changes reveal different transcriptional responses in the larvae of the bark beetle *Dendroctonus rhizophagus* during the cold season. *Sci Rep* (2026). <https://doi.org/10.1038/s41598-026-40764-4>

Moises Becerril, Gerardo Zúñiga, Verónica Torres-Banda, María-Fernanda López, Claudia Cano-Ramírez, Gabriel Obregón-Molina & J. Manuel Quijano-Barraza

We are providing an unedited version of this manuscript to give early access to its findings. Before final publication, the manuscript will undergo further editing. Please note there may be errors present which affect the content, and all legal disclaimers apply.

If this paper is publishing under a Transparent Peer Review model then Peer Review reports will publish with the final article.

Temperature changes reveal different transcriptional responses in the larvae of the bark beetle *Dendroctonus rhizophagus* during the cold season

Moises Becerril<sup>1</sup>, Gerardo Zúñiga<sup>1,\*</sup>, Verónica Torres-Banda<sup>1</sup>, María-Fernanda López<sup>1</sup>, Claudia Cano-Ramírez<sup>1</sup>, Gabriel Obregón-Molina<sup>1</sup> and J. Manuel Quijano-Barraza<sup>1</sup>

<sup>1</sup>Laboratorio de Variación Biológica y Evolución, Departamento de Zoología, Escuela Nacional de Ciencias Biológicas, Instituto Politécnico Nacional, Prolongación de Carpio y Plan de Ayala s/n, Miguel Hidalgo, Ciudad de México, CP 11430, México.

\*Correspondence: E-mail address: gzunigab@ipn.mx

## Abstract

Bark beetle, *Dendroctonus rhizophagus*, colonises and kills healthy sapling pine trees in the Sierra Madre Occidental, Mexico. In the autumn, its fifth-instar larvae migrate to the host's roots (hibernaculum) to overwinter; however, little is known about temperature changes in this hibernaculum during the cold season and the physiological responses related to cold tolerance in this species. A three-year temperature record was analysed to define thermal thresholds throughout the cold season in the hibernaculum. Fifth-instar larvae were collected from the thermal thresholds and sequenced using RNA-seq to assemble a global *de novo* transcriptome. Differential expression, gene enrichment and co-expression analyses were performed to determine the main metabolic pathways and biological processes taking place in these larvae during the cold season. Three thermal thresholds were defined: late-fall, mid-winter and late-winter. In late-fall, the transcriptional response was related to motility and feeding, possibly associated with the migration of larvae to the hibernaculum; in mid-winter, it was related to the physiological adjustments involved in the cold resistance phenotype; and, in late-winter, it was related to the processes involved in pupal chamber construction and the onset of metamorphosis. Our results show that the temperature in the hibernacula and the transcriptional response of fifth-instar larvae of *D. rhizophagus* change during the cold season, where lower temperatures coincide with the cold resistance phenotype.

**Keywords:** *Dendroctonus rhizophagus*; cold-hardiness; transcriptomics; DEGs; co-expression; larvae

## Introduction

Molecular processes form the basis for understanding the physiological, morphological, and behavioural adaptations that individuals display at different spatial and temporal scales [1, 2]. Abiotic factors act as selective pressures that influence genetic variability, phenotypic plasticity, and organismal adaptation [2]. In the case of holometabolous insects, different abiotic factors can act independently or synergistically in each developmental stage, because they are quasi-independent modules that express specific phenotypes despite their progression over time [3, 4]. For example, the length of developmental stages (eggs, larvae, pre-imago, and adults) and life cycle (univoltine or multivoltine) are largely influenced by climatic variables and factors such as temperature, photoperiod and food quality [5], whose variation, intensity, and persistence in each developmental stage affect survival [1, 6, 7].

Low temperatures have widespread effects on the physical fitness of insects. They significantly reduce enzymatic activity, metabolic rate, and other vital functions, such as neuromuscular activity, which affect mobility and flight capacity, breakdown of accumulated energetic reserves, organism growth and maturation,

and the duration of developmental stages, life cycle, and number of generations of the species [8]. Overwintering insects inhabiting cold and temperate regions overcome low temperatures or freezing through functional adaptations that optimise their survival through three primary strategies: freeze tolerance, freeze avoidance, and chilling intolerance [9]. Freeze-tolerant insects can survive ice formation in their bodies when the corporal temperature drops below 0°C; however, it is restricted to the extracellular compartments, avoiding intracellular freezing through osmotic and mechanical processes, as it has been reported to species that inhabit high latitude environments with harsh winter conditions [9-11]. In contrast, freeze-avoidance insects can survive in low temperatures by maintaining the haemolymph in liquid state, thereby avoiding ice formation in the entire body; this way, the insects remain chilled at subzero temperatures. However, chill-intolerant insects cannot survive the direct effects of low temperatures without internal ice formation [9-13]. Although these strategies present common physiological and biochemical responses, as the synthesis of low molecular weight cryoprotectants such as polyols and sugars, free amino acids, and ice binding proteins (IBPs), their expression depends on the severity of winter conditions associated with latitude, altitude, habitat, and organismal capacities, which vary among species, populations, and developmental stage [14-17].

Two overwintering strategies, at least, have been observed in bark beetles (Curculionidae: Scolytinae). The first in species with a high cold tolerance, both in adults and larvae, allowing the different stages to survive the winter under the bark, where they feed off the phloem of host trees without migrating to other sites. The second strategy, found in species with limited cold tolerance, involves a behaviour where adults and larvae migrate to the forest floor to overwinter [14]. *Dendroctonus* bark beetles are a Holarctic taxon composed of 21 species, 19 of which are distributed along the coniferous temperate forests of North and Central America and two across the boreal regions of Europe and Asia [18, 19]. Their life cycle can be either univoltine or multivoltine and their development occurs almost exclusively under the bark of host trees, except for a brief dispersal period. The life cycle of these bark beetles is strongly influenced by temperature, because high temperatures increase the growth rate and reduce the development time, whereas low temperatures produce the opposite effect in species with wide distribution ranges in North and Central America, such as *D. valens*, *D. ponderosae*, *D. frontalis* and *D. rufipennis* [14, 20-23].

Studies related to cold hardiness in *Dendroctonus*-bark beetles have been performed on species distributed in latitudes > 35° N, such as *D. ponderosae*, *D. armandi*, *D. rufipennis*, *D. frontalis* and *D. valens* from China, where it was recently introduced [14, 21-30]. The responses of these species to low temperatures vary; for example, the larvae of *D. armandi* present low cold tolerance in November when they are exposed to temperatures between 5.4°C and -5.7°C, while larvae have higher cold tolerance at lower temperatures (-10°C) in December. The tolerance change matches with the increase in synthesis activity and accumulation of cryoprotective molecules such as sorbitol, trehalose, glycerol, and anti-freezing proteins reaching their highest concentrations under colder conditions (December-January) [31, 32]. Several studies, ranging in location from the southern United States of America to Canada, have evaluated the cold response of *D. ponderosae* at distinct developmental stages. These studies have shown that the supercooling point of adults of this species varies over months, being between -28.7°C and -40°C [24, 33], thereby demonstrating a correlation between the temperature decrease and metabolic rate, as well as the synthesis of cryoprotectant molecules [22, 34]. In *D. frontalis*, it has been reported that individuals do not survive temperatures below -17° C, even though this species is exceptionally well adapted to low temperatures, which limits its distribution range [14, 35, 36]. Recently, transcriptomics, proteomics and metabolomics studies conducted on *D. ponderosae*, *D. valens* and *D. armandi* have expanded our knowledge of the physiological changes experienced by these insects during the cold season. In these studies, differentially expressed genes related to HSPs, immune responses, cuticle synthesis, DNA repair, detoxification, and antioxidant gene synthesis in larvae and adults during the cold season were reported [22, 24, 26-29].

*Dendroctonus rhizophagus* (Thomas & Bright) is a species endemic to the Sierra Madre Occidental (SMOc) in northwestern Mexico. Its life cycle is univoltine and synchronous; however, in contrast with other members of the genus, it colonises healthy pine seedlings ( $\geq 1.5$  cm diameter base), and saplings ( $< 8$  cm in diameter at 1.4 m height and  $< 3$  m tall). The emergence of adult insects begins in early summer, matching the onset of the rainy season. In contrast with other *Dendroctonus* species which aggregate in tens to hundreds of pairs to attack host trees, only one or two couples of *D. rhizophagus* colonise a single host. Once a couple colonises a tree, they copulate and build a gallery where the females oviposit. Larval stages, from the first to fifth instar, develop from mid-summer to late fall in the host stem; however, in late fall, the fifth instar larvae migrate towards the hibernaculum, where they spend the entire winter. The following year, these larvae transform into pupae in early spring, then into pre-imagos, and finally, adults emerge in early summer [37].

The larval migration of *D. rhizophagus* towards the hibernaculum in the sapling roots is a compensatory strategy that mitigates the effect of winter temperature, as has been reported in *Ips pini* and some populations of *I. grandicollis* that migrate to the leaf litter beneath the host tree to overwinter [14]. Based on historical records of temperature and humidity variations in the SMOc, we hypothesised that the temperature in the larval hibernaculum varies throughout the cold season, triggering different physiological responses from the time when larvae begin their migration until they prepare for the pupal stage as the winter season progresses. We determined three thermal thresholds in the hibernaculum during the cold season: late fall (November), midwinter (January), and late winter (February). The transcriptional response of these larvae is a dynamic and complex process in these thermal thresholds, involving the activation of different metabolic pathways mainly related to muscle activity, energy production and administration, and cellular cryoprotection, as well as other compensatory mechanisms as immune response and protein homeostasis that help maintain and adjust the transcriptional response in a changing cold season environment. This information is crucial for the development of novel and more specific integral management strategies using molecular-based techniques, such as gene silencing, as has been assayed in other bark beetles and insect species [38-40].

## 2. Results

### 2.1. Temperature record

We found significant differences between the larval hibernaculum and stem mean temperatures (mT) across the three years in the cold season ( $t = 6.45$ ,  $p < 0.001$ ; Table S1). The mT in the larval hibernaculum was higher and less variable than that in the stem (Figure 1A, Table S1). In the hibernaculum and stem, the mT values were consistently lower during December-January than in the other periods (Figure 1B). The mean minimum temperature (mT<sub>min</sub>) variation per month, across the three years during the cold season on the hibernaculum varied from 3.32°C in November to -2.80°C in January; meanwhile, the mT<sub>min</sub> on the stem changed from -4.45°C in November to -17.33°C in January (Table S1). All pairwise comparisons of the monthly hibernaculum temperatures were statistically different (ANOVA,  $F = 434.7$ ,  $df = 2376$ ,  $p < 0.001$ ; Table 1), except for the comparison between December and January ( $p = 0.9248$ ) (Table 1, S2). As there were no statistical differences in the mT<sub>min</sub> between December and January, we selected January as the collection point because this month had the lowest recorded temperature.

### 2.2. Transcriptome assembly

In total, 123 825 178 clean reads [41 500 952 to late-fall (Nov), 38 942 681 to mid-winter (Jan), and 43 381 545 to late-winter (Feb)] were obtained. We assembled a *de novo* transcriptome with clean reads of the three thermal thresholds of the fifth instar larvae of *D. rhizophagus*. From this assembly we obtained 48 039 unigenes with an N50-value of 3893 nucleotides (nt), 26.14% of which were found in the range of 1001 to 3000 nt (Figure S1), which is slightly longer than that for other bark beetles [28]. BUSCO analysis of the *de novo* assembly showed that  $> 97\%$  of the cleaned reads properly matched the assembly (Table S3), similar to the assemblies of other bark beetles [28]. From the 2124 genes included in the

endopterygota\_odb10 database, 95.6% were found in the fifth instar larval transcriptome as complete genes, 1.4% were fragmented, and 3% were missing (Figure S2). Moreover, 81.99% of the unigenes had the best alignment hit (E-value of  $1e^{-20}$ ), with 70% coverage of the proteins identified in the *D. ponderosae* genome (Table S4).

### 2.3. Differential expression and enrichment analysis

Principal component analysis (PCA) showed that the biological replicates at each thermal threshold were homogeneous, no outliers were found (Table S5, Figure S3A, S4), where PC1 and PC2 accounted for 34.53% and 27.18% of the total variation, respectively. After differential expression analysis, 1668 differential expressed genes (DEGs) were identified among the thermal thresholds (Figure 2A, S5). The numbers of upregulated and downregulated genes were 522 and 386 (late fall vs. mid-winter), 460 and 435 (mid-winter vs. late winter), and 182 and 161 (late fall vs. late winter), respectively (Figure 2B, S5).

Based on the enrichment analysis of the DEGs, we identified different Gene Ontology (GO) terms and Kyoto Encyclopaedia of Genes and Genomes (KEGG) orthologous groups at each thermal threshold in the fifth-instar larvae of *D. rhizophagus* (enrichment of down-regulated genes are included in Figures S6, S7, S8). In the late fall larvae, the most representative GO terms, and KEGG orthologous groups were 'sphingomyelin catabolic process (GO:0006685)', 'ceramide biosynthetic process (GO:0046513)', and 'guanine nucleotide-binding protein G(o) subunit alpha (K04534)' (Figure 3 and S9, Table S6, S7). In the mid-winter larvae, the transcriptional response was related to the 'hydrogen peroxide biosynthetic process (GO:0050665)', 'glycogen phosphorylase activity (GO:0008184)', 'phosphoenolpyruvate carboxykinase (GTP) activity (GO:0004613)', 'E3 ubiquitin-protein ligase HECW2 (K12168)', 'G protein-coupled receptor MTH (Methuselah protein) (K04599)', and 'adenylate cyclase 1 (K08041)' (Figure 3, S10, Table S8, S9). Finally, in late winter larvae, the response was related to the 'carbohydrate metabolic process (GO:0005975)', 'cellulase activity (GO:0008810)', 'cellulase catabolic process (GO:0030245)', 'adenylate cyclase 1 (K08041)', and 'calmodulin-regulated spectrin-associated protein (K17493)' (Figure 3, S11, Table S10, S11).

### 2.4. Co-expression network analysis

PCA showed clear separation among the transcriptional responses of larvae associated with the three thermal thresholds. Biological replicates within each thermal threshold clustered together, indicating a homogeneous transcriptional response and experimental reproducibility (Figure S3B). PC1 and PC2 explained 53.6% and 34.38% of total variation, respectively. Consequent upon the co-expression network analysis, eleven modules were recovered (hereafter referred to by colour as portrayed in Figure 4), of which only modules 'Blue', 'Gray', 'Green', 'Red', 'Midnightblue', and 'Pink' showed significant positive correlations (Figure 4), that is, gene expression levels within each of these modules are positively correlated (co-expressed), allowing for the identification of relevant hub genes within biological processes for each thermal threshold.

From the modules above, the 'Blue' (0.84,  $p < 0.005$ ), 'Gray' (0.87,  $p < 0.005$ ), 'Green' (0.82,  $p < 0.005$ ), and 'Red' (0.67,  $p < 0.05$ ) modules showed positive correlation values in the gene expression level in the late fall thermal threshold (Figure 4, S12A). A total of 12 hub genes were identified in these modules: five in 'Blue' ( $k_{\text{Within}} = 32.72\text{-}33.87$ ), four in 'Green' ( $k_{\text{Within}} = 16.34\text{-}16.80$ ), and three in 'Red' ( $k_{\text{Within}} = 17.84\text{-}18.71$ ) (Figure 5, Table S12). The enrichment analysis of genes assigned to these five modules resulted in 46 GO terms (Table S13), highlighting those from biological process category related to energy obtention, such as 'cellulose catabolic process (GO:0030245)', 'fructose 2, 6 biphosphate metabolic process (GO:0006003)', 'fructose metabolic process (GO:0006000)', and 'carbohydrate metabolic process (GO:0005975)', as well as chemical communication such as 'odorant binding (GO:0005549)'. Among the 17 KEGG orthologous groups, we found those related to organizational and contractile apparatus of the muscle such as the KEGG orthologue term 'Titin (K12567)', protein

homeostasis as 'HSP70 (K03283)', and carbohydrate metabolism as 'beta-galactosidase (K25543)', 'cathepsin (K01365)', and 'polygalacturonase (K01184)' (Figures 5, S12A, Table S13).

At the mid-winter thermal threshold, only the 'Midnightblue' module showed a positive correlation (0.81,  $p < 0.005$ ) at the gene expression level, and 36 hub genes were found ( $k_{\text{Within}} = 152.86$ ; Figures 5, S12B, Table S12). The enrichment analysis resulted in 31 GO terms (Table S13), including 'translation (GO:0006412)', 'proteosomal ubiquitin-independent protein catabolic process (GO:0010499)', and 'ferroxidase activity (GO:0004322)', as well as four KEGG orthologous groups, highlighting 'ferritin heavy chain (K00522)', 'crystalin, alpha B (K09542)' and 'stearoyl-CoA desaturase (K00507)' related to protein catabolism, oxidative stress, and lipid metabolism (Figures 5, S12B, Table S13).

Finally, in the late-winter thermal threshold (Feb), the 'Pink' module presented significant positive correlation (0.67,  $p < 0.05$ ; Figure 4) in the gene expression level with five hub genes ( $k_{\text{Within}} = 13.68-15.17$ , Table S12). The enrichment analysis resulted in 18 GO terms, including molecular function related to carbohydrate metabolism as 'cellulose activity (GO:0008810)', 'cellulose catabolic process (GO:0030245)', 'cellulose 1, 4-beta cellobiosidase activity (GO:0016162)'. Among the six enriched KEGG orthologous groups, some were related to fatty acid biosynthesis [*e.g.* fatty acid synthase, animal type (K00665)], protein homeostasis [*e.g.* heat shock 70kDa protein(K03283)], and carbohydrate metabolism [*e.g.* pectinesterase(K01051)] (Figures 5, S12C, Table S13).

### 3. Discussion

In this study, we aimed to evaluate the transcriptional response of fifth instar larvae of the bark beetle *D. rhizophagus* throughout the cold season. We found significant differences in the mean temperatures ( $mT$ ) and mean minimum temperature ( $mT_{\text{min}}$ ) between the hibernaculum and stem and among thermal thresholds: late-fall, mid-winter, and late-winter (Figure 1; Table S1), with the second being colder than the first and third. While the environmental temperature showed a higher variation during the cold season, it was lower in the hibernacula. These three thermal thresholds, which matched the changes in the environmental temperatures, were identified. Our findings showed a differential transcriptional response of the larvae related to temperature changes at these thermal thresholds. At the late-fall threshold, the transcriptional response was related to motility and feeding, possibly associated with larval migration towards the hibernaculum in the roots of tree saplings, where they overwinter. At the mid-winter threshold, it was related to physiological readjustments involved in the cold-hardiness phenotype. Finally, at the late winter threshold, the transcriptional response was linked to processes possibly involved in the beginning of metamorphosis, feeding, and motility of the larva. These transcriptional responses could be mechanisms that tightly regulate the physiological responses of the fifth instar larvae of *D. rhizophagus*, as has been documented in many insect species, including some *Dendroctonus* species [23, 28, 29, 32].

**Late fall (November) larvae.** The most important biological event in the late-fall thermal threshold is the migration of fifth-instar larvae towards the hibernaculum. Underground migration has been documented in different overwintering beetles [41-44]; it is a complex phenomenon that can be driven by different processes, such as chemotaxis, thermotaxis, hygrotaxis, thigmotaxis, phototaxis, and geotaxis [45-49]. We propose that *in-situ* migration of *D. rhizophagus* larvae could be mainly driven by thermotaxis and possibly by chemotaxis, as suggested by our results, given the differences and relatively low variation in temperature between the hibernaculum and stem. Although migration is uncommon in bark beetles and *Dendroctonus* species, some studies on *Ips paraconfusus*, *I. typographus*, and *D. ponderosae* have reported thermotaxis and chemotaxis as migration triggers [14, 50, 51]. However, further studies are required to test this hypothesis. Thermotaxis is a process regulated by signalling cascades which could involve the activation of metabotropic receptors such as the transient potential receptors

(TPRs) and glutamate receptor-like channels (GLRs), rhodopsin, the alpha subunit of G-proteins (G- $\alpha$ ), and phospholipases [52]. Through enrichment and co-expression analyses, we identified metabotropic receptors in the transcriptome. Thus, the presence of TPRA1, TPRL, and GLR-3 receptors in the transcriptome coupled with overexpression of the gene encoding guanine-nucleotide binding protein G (o) subunit alpha (G $\alpha$ o; Figure 3, Table S6, S14) suggests that migration probably is mediated by thermotaxis. The gene encoding G $\alpha$ o has also been found up-regulated in the larvae and adults of the bark beetle *D. valens* exposed to low temperatures [28]. In addition, these metabotropic receptors bind to signalling molecules [53] and activate G proteins, which may trigger intracellular responses via second messengers and regulate diverse biological processes such as sensory perception, nervous system, immune system regulation, and behaviour [52, 54]. Hence, the TPRs and GLRs found in *D. rhizophagus* are potentially involved in cold avoidance and thermotaxis, as reported for TPRA1, TPRL, and GLR-3 in *Drosophila melanogaster* [55] and *Caenorhabditis elegans* [56], respectively. The low expression of these receptors in the transcriptome of *D. rhizophagus* fifth instar larvae (Table S15) could be explained by the use of whole-body larvae (composite structures), which may mask tissue-specific gene expression [57]. Experiments focusing on the expression of TPRA1, TPL, and GLR-3 during thermotaxis must be conducted in the late fall larvae of *D. rhizophagus*.

The chemotaxis could also be involved in the migration of the late fall larvae, as suggested by the GO term 'odorant binding' of the 'Blue' module of the co-expression analysis (Figure 5, Table S13). Ongoing studies performed by our team indicate that the gregarious behaviour of fifth-instar larvae of *D. rhizophagus* could be mediated by aggregation pheromones [Cano-Ramírez personal communication], as has been demonstrated in the larvae of bark beetles *D. micans* and *D. punctatus* [58, 59]. We hypothesised that migration towards the hibernaculum of fifth instar larvae could also be mediated by pheromones, because this must be synchronised and orderly owing to the limited space between the sapwood and bark of the stem and the roots from saplings. In this context, odorant binding proteins (OBPs) might play an important role in the aggregation and migration of *D. rhizophagus* larvae towards hibernaculum because they are essential for the recognition of aggregation pheromones, as has been demonstrated in the larvae of lepidopteran species, which have been reported to have different chemosensory receptors and OBP's, among other proteins [60-63]. Future studies with specific experimental designs should be conducted to test the participation of these chemoreceptors in the migration of the larvae of *D. rhizophagus*.

Among other important aspects associated with the migration of fifth instar larva of *D. rhizophagus* is obtaining energy through feeding to build the gallery towards the hibernaculum. Our co-expression networks revealed the presence of some GO terms and KEGG orthologous in the 'Red' module related to carbohydrate metabolism and one KEGG ortholog associated with locomotion ('titin') (Figure 5, Table S13). Titin (TTN) could be a key protein involved in muscle contractility during insect migration and *in situ* movement. [64], because this protein enhances muscle strength [65]. Among the GO terms are 'cellulose activity', 'cellulose catabolic process', 'cellulose 1, 4-beta-cellobiosidase activity' (Figure 5, Table S13), as has been observed in fourth instar larvae and callow of *D. rhizophagus* [Quijano, personal communication], bark beetles *D. ponderosae* [24], *I. typographus* [66, 67], and curculionid *Diabrotica virgifera virgifera* [68], which are species that do not migrate, during the construction of their galleries.

Finally, the up-regulated (*e.g.*, sphingomyelin phosphodiesterase, SMPD) and co-expressed gene in the 'Green' module as hub gene (apolipoprotein, apoLp) related to cell membrane maintenance and lipid transport, suggests the onset of late-fall larvae acclimation to cold resistance. It is known that SMPD promotes changes in cellular membrane composition to produce ceramides via endosome and lysosome activity [69], whereas apoLp is involved in lipid transport, including cholesterol (Figure 3, Tables S6, S12, S14). Both proteins regulate osmolarity in haemolymph insects that face cold environments, thereby increasing both membrane permeability and fluidity [70, 71]. These modifications may maintain signalling processes, protein domain distribution in the membrane, cholesterol homeostasis,

and cell differentiation [72-74], as has been reported in laboratory studies performed with *Locusta migratoria* and *Drosophila montana* [75, 76]. Further experiments are required to verify the participation of these proteins in the modification of the cellular membranes under cold conditions in *D. rhizophagus* larvae.

**Mid-winter (January) larvae.** At this thermal threshold, which corresponds to the coldest phase, the larvae settled in the hibernaculum. The transcriptional responses of the DEGs and co-expressed genes in the 'Midnightblue' module were related to cold resistance, including lipid and carbohydrate metabolism, response to reactive oxygen species (ROS), and proteostatic processes (Figures 3, 5, Tables TS8, S12, S13, S14). Most genes involved in these processes have been reported to be upregulated in *D. ponderosae*, *D. valens* and *D. armandi*, as well as in other insect species [24, 28, 31] during the cold season. Within lipid metabolism, we identified genes encoding the elongation of very long saturated fatty acid protein 7 (ELOVL7) and stearoyl-CoA 9 desaturase (SCD) (Figure 3; Tables S8, S12 and S14). ELOVL7 catalyses the addition of carbon atoms to fatty acid saturated chains to produce very long fatty acids (VLSFAs) (>20 carbon), which are precursors of other lipids such as ceramides, sphingolipids, and cholesterol esters, and participate in other vital processes such as membrane composition and fluidity, lipid droplet formation, and the lipid signalling pathway [77-79]. SCD converts VLSFAs into very long unsaturated fatty acids (VLUFAs) and other unsaturated fatty acids (UFAs) and monounsaturated fatty acids (MUFAs) which are easily transported to different tissues under cold temperatures [78].

Unsaturated fatty acids (including VLUFAs) and MUFAs participate in the maintenance of cell membrane structure via glycerophospholipid (GPLs) synthesis (*e.g.* phosphatidylcholine, phosphatidylethanolamine, phosphatidylserine, and phosphatidylinositol) [70, 79]. The upregulation of genes encoding ethanolamine kinase (ETNK, Table S14) and glycerol kinase (GK) (Figure 5, Table S12, S14) may be associated with the synthesis of GPLs in the fifth instar larvae of *D. rhizophagus*. GK catalyses the conversion of glycerol to glycerol-3-phosphate, the backbone of phosphatidic acid and the precursor of GPLs [79], whereas ETNK may increase the synthesis of phosphatidylethanolamine in overwintering insects, preventing the solidification of cellular membranes during cold stress [71, 80, 81]. Finally, the presence of the hub gene encoded serine palmitoyltransferase 2 (SPTLC2) (Figure 5, Table S12), suggesting the synthesis of sphingolipids, which might be related to cellular membrane formation in the fifth instar larvae of *D. rhizophagus*, as it has been documented in the Colorado potato beetle (*Leptinotarsa decemlineata*) under cold conditions [69, 81-83].

Lipids also play a crucial role in obtaining energy in overwintering insects via  $\beta$ -oxidation of VLSFAs [70, 72, 84]. The up-regulation of the gene encoding peroxisomal acyl-coenzyme A oxidase (ACOX) in the mid-winter larvae of *D. rhizophagus* suggests that this pathway is active (Figure 3, Table S8, S14), because this enzyme regulates and controls the  $\beta$ -oxidation from which are produced short, medium, and long chain fatty acids. These fatty acids are catabolised to produce acetyl-CoA and acyl-CoA via  $\alpha$ -oxidation, which can be later used in the tricarboxylic acids cycle (TCA) where some intermediates, such as glycerol, can participate in the gluconeogenesis pathway to produce glucose as an energy resource or as an intracellular cryoprotectant, in the GPLs synthesis as a membrane component (as was mentioned earlier), and as a cryoprotectant molecule [79, 84-86].

Similar to GPLs synthesis, our results support that the gluconeogenesis is an active pathway in the fifth instar larvae of *D. rhizophagus*, owing to the up-regulation observed in the pyruvate carboxylase (PC) encoding gene, the up-regulation and presence of the genes encoding phosphoenolpyruvate carboxykinase (PEPCK) and fructose-biphosphate aldolase-like (FBA-like) in the 'Midnightblue' module (Figure 3, Tables S8, S12, S14). The presence of the enriched GO term related to adenosine triphosphate (ATP) synthesis (Figure 5, Table S13) suggests that glucose can be used as an energy source, as has been suggested in the bark beetles *D. ponderosae* and *D. valens*, other insects such as *Sarcophaga bullata* and other arthropod groups under cold conditions [27, 87-89]. However, the production of glucose in the fifth

instar larvae of *D. rhizophagus* may also occur via glycogenolysis, as suggested by the upregulation of the gene encoding glycogen phosphorylase (GP) (Figure 3, Table S8, S14). Both pathways have been related to glucose availability in the bark beetles *D. ponderosae* and *D. valens*, as well as in insects of boreal latitudes, such as *Belgica antarctica* [27, 28, 90].

Glycerol, a cryoprotectant molecule, is vital for maintaining the liquid state of the haemolymph and preventing cellular and tissue damage during cold periods [27, 88, 89, 91]. The upregulation of the gene encoding GK, as described above, and the presence in the transcriptome of the genes encoding glycerol-3-phosphate dehydrogenase (GPDH) and triosephosphate isomerase (TPI), which were not differentially expressed (Table S15), suggest that glycerol could play a cryoprotectant role in the fifth instar larvae of *D. rhizophagus*. The same conclusion was drawn from experimental assays conducted under cold conditions in *D. ponderosae*, *D. armandi*, and *Glenea cantor* [27, 31, 92]. Nevertheless, future studies should be conducted to determine whether other molecules, in addition to glycerol, can act as cryoprotectants in the fifth-instar larvae of *D. rhizophagus*.

Another important set of genes found in mid-winter larvae include genes encoding heat shock proteins (sHSPs, HSP60, HSP70, and HSP90). In insects, these proteins participate in the modulation of the immune system, protein homeostasis, abiotic and biotic stress, and development [93, 94]. In this context, our results showed the upregulation of genes encoding the heat shock factor (HSF) and dual oxidase (DO) which may be associated with immunity (Table S14). HSF regulates the expression of several HSPs in insects and modulates the expression of proteins involved in immunological pathways such as IMD, Toll, and Jak/STAT, which are involved in the recognition of gram-negative bacteria, fungi, and viruses [94, 95]. DO is related to the production of hydrogen peroxide (H<sub>2</sub>O<sub>2</sub>) required to produce hypochlorous acid (HOCl), a microbicidal agent that participates in microbiota equilibrium in the gut and resistance to foreign microorganisms, as has been demonstrated in *Bactrocera dorsalis* and *D. melanogaster* adults [96-99].

DO activity and the presence of a small HSP in the fifth instar of *D. rhizophagus* suggested a homeostatic process involving different proteins. The DO generates reactive oxygen species (ROS; e.g. lipid peroxides, aldehyde products, reaction intermediates and protein carbonyls) that affect protein structures producing proteotoxicity [100], which is counteracted by the action of the sHSPs (e.g., alpha-crystallin B chain) and other HSPs activated by the HSF present in the 'Midnightblue' module and the GO term 'chaperone-mediated protein folding' and the KEGG process 'Crystallin, alpha B' (Tables S13, S14) involved in the proteostasis as suggested in other insects and bark beetles, including *D. valens* and *D. ponderosae* [22, 28, 29, 82, 101, 102]. The study and characterisation of HSPs in insect pests such as bark beetles reveal potential for the development of RNAi as a *Dendroctonus*-specific management tool against rapidly expanding bark beetle populations, as has been assayed in species from this genus [38, 39]. Although HSPs can reduce the effects of ROS, other proteins can neutralise the activity of these molecules. Our results showed the expression of genes that encode proteins with antioxidant activities (ferritin (FTH1) subunit, ferritin heavy polypeptide-17 (FTHL17; Figure 3, Table S8, S14) and the presence of hub genes (glutathione-S transferase (GST), peroxiredoxin-1 (PRDX1), and FTH1 subunit) in the 'Midnightblue' module (Figure 5, Tables S8, S12, S13), as have been documented in other boreal insect species under harsh environmental conditions [103-105].

Other complementary elements necessary to avoid proteotoxicity were found in the larvae of this thermal threshold, such as the up-regulated genes encoding enzymes of the ubiquitin proteolytic system (UPS) (e.g., E3 ubiquitin-protein ligase HEW (HUWE1), ubiquitin thioesterase traid (TRABID), and ubiquitin-like modifier-activating enzyme (UBA); Figure 3, Table S8, S14). UPS enzymatic pathway, reported for other insects, is involved in the degradation or preservation of cellular proteins that identify, mark, and degrade harmful protein aggregations and misfolding proteins under oxidative and thermal stress [106, 107], our results suggest that this process may be active in the fifth instar larvae of *D. rhizophagus*. In addition, this system and the HSPs enzymes are involved in other cellular

processes, such as DNA repair, cell cycle regulation, antigen presentation, cell-cell communication, cell differentiation and apoptosis [82, 106, 107].

Other relevant elements potentially associated with larval acclimatation at this thermal threshold were the upregulated genes encoding G-protein coupled receptor Mth 2 (GPCR<sub>mth2</sub>), inositol polyphosphate 5-phosphatase (IPP5P), and Ca<sup>2+</sup>/calmodulin-responsive adenylate cyclase (ADCY) (Figure 3, Table S8, S14). These proteins participate in signal transduction and trigger pathways related to environmental stress, as demonstrated in *D. melanogaster* and *Spodoptera litura* under cold conditions [108-112]. Because these genes and enzymes have not been documented in other studies on bark beetles under environmental stress, we hypothesised that the DEGs encoding GPCR<sub>mth2</sub>, IPP5P, and ADCY in *D. rhizophagus* could be involved in the cold sensation, starvation, and damage produced by oxidative stress. Future studies should be performed to demonstrate the functional role of this set of enzymes in the fifth instar larvae of this bark beetle under cold conditions. Lastly, the upregulation of cytochrome P450 family 6 (*e.g.* CYP6DJ1, CYP345E2, and CYP6DG1; Figure 3, Table S8, S14) suggests that the larvae in the hibernaculum carry out the degradation of xenobiotic compounds produced by the host tree (*e.g.* monoterpenes and diterpenes), which penetrate the larvae through the cuticle, feeding, or inhalation. Broadly documented experimental evidence reveals that these CYPs in *Dendroctonus* species participate in the detoxification of terpenoid compounds [113-116]; however, given the functional diversity of CYP450, their probable participation in other metabolic pathways in the fifth instar larvae of *D. rhizophagus* cannot be disregarded.

**Late winter (February) larvae.** At this thermal threshold, larvae display a transcriptional response potentially involved in the preparation of larval-pupal metamorphosis, involving feeding and larval movement during pupal chamber construction. In holometabolous insects, the energy obtained by feeding at the last larval instar is essential for inducing the synthesis of hormones, such as prothoracic hormone (PTTH), which is necessary for continued development [117, 118]. Pupal chamber construction and metamorphosis in bark beetles require energy that could be acquired by larvae through the degradation of structural and stored carbohydrates present in the sapling phloem, as suggested by the presence of glycosyl hydrolase genes (GHs) (*e.g.* exoglucanases (ExGs), endoglucanases (EG), beta-galactosidase-1-like (GLB1-like), rhamnogalacturonase lyase (RGL)). In addition, energy is obtained from stored carbohydrate metabolism during the larval stages, as the overexpression of the gene encoding the glycogen debranching enzyme (GDE) suggests that glucose molecules may be obtained by glycogenolysis (Figure 3, Table S10, S14) [119]. Other energy sources may originate from fatty acid metabolism as suggested by the gene encoding fatty acid synthase (FAS). Collectively, the DEGs, GO terms, KEGG orthologous groups, and co-expressed genes in the 'Pink' module (Figures 3, 5; Tables S10, S12-S14) indicate that obtaining energy through feeding or metabolising stored reserves is essential in the fifth-instar larvae of *D. rhizophagus* at this thermal threshold.

The movement of bark beetle larvae during pupal chamber construction involves muscular contractions. In this context, the DEGs encoding the muscle M-line assembly protein unc 89 (UNC-89), cadherin-87A (Cad87A), filamin-A (FLNA), TTN, protein muscleblind (MBNL), and neural-cadherin (NCAD) suggested that this process is active in fifth instar larvae (Figure 3, Table S10, S14). Furthermore, as suggested by the upregulation of ankyrin (ANK) and sarcomere proteins, muscle movement and contraction may be involved in muscle fibre repair in fifth instar larvae [119-121]. Movement, contraction, and muscle repair are processes that occur during pupal chamber construction in bark beetles, while fifth-instar larvae of *D. rhizophagus* construct their pupal chambers by slightly invading the xylem of sapling roots. Other *Dendroctonus* species whose larvae do not migrate build the pupal chamber in the intracortical region of mature tree stems, which involves the horizontal migration of the larvae from the cambium to the outer bark of the tree [122].

Conclusions

We found changes associated with different physiological processes in fifth-instar larvae of *D. rhizophagus* across three thermal thresholds (late fall, mid-winter, and late winter) in the cold season. In late fall, the main transcriptional responses were related to thermotaxis, chemotaxis, and feeding, which are necessary for the construction of the gallery to reach the hibernaculum, where temperatures are warmer and less variable than those of the stem during the cold season. In mid-winter, the coldest temperatures were recorded in the hibernaculum during the cold season, and the transcriptional response of larvae settled in this refuge was related to cold-hardiness, possibly under the cold avoidance strategy, from which we highlight the use of lipids for the maintenance of cell membranes, the energy obtention from lipids and carbohydrates, and other important processes related to the immune response, proteostasis, and the response to ROS. Lastly, in late winter, the transcriptional response was related to feeding, motility, and energy obtention during the construction of the pupal chamber and continuation of development.

#### 4. Materials and methods

##### 4.1. Temperature variation and larvae collection

To determine the variation in mean ( $mT$ ), minimum ( $mT_{\min}$ ), and maximum ( $mT_{\max}$ ) environmental temperatures from November to February during the cold season, we analysed historical records of these temperatures from 2010 to 2018 in the Guachochi municipality, Chihuahua state (No. 00008312 station, National Weather Service, Chihuahua, Mexico). In addition, we recorded the hourly temperature at the larval hibernaculum and stems of three different saplings of Durango pine (*Pinus duranguensis*) during three consecutive years (2019–2020, 2020–2021, 2021–2022). Three data loggers (HOBO by ONSET, USA) were placed at 30 cm beneath the soil surface along with larval hibernaculum and three others at 20 cm above the soil surface over stems of these sampling at Agua Blanca locality, Guachochi municipality, Chihuahua state, Mexico (26°47'22' N, 107°15'49.12' W). As the daily temperature records obtained by the three data loggers in the hibernaculum and stems of the saplings were independent, we estimated the  $mT$ ,  $mT_{\min}$ , and  $mT_{\max}$  at each level as follows: three records/h  $\times$  24 h  $\times$  number of days per month (Table S1). From both datasets, three thermal thresholds (lowest temperatures recorded in a specific period of time from November to February) were recognised in the cold season, hereinafter referred to as 1) late fall, 2) mid-winter, and 3) late winter.

To determine the specific collection points of the fifth instar larvae of *D. rhizophagus* in late fall, mid-winter, and late winter, we constructed two climograms with the temperature data recorded from three data loggers during the three years of study at the hibernaculum and stem. The first climogram was constructed with the mean temperature at each level, and an independent samples  $t$ -test was used to evaluate the significant differences between them. The second climogram was constructed using the mean, minimum, and maximum temperatures per day to show the temperature variation only in the larval hibernaculum. To evaluate temperature changes in the hibernaculum from November–February of the years 2019–2020, 2020–2021 and 2021–2022, were calculated and, one way-ANOVA and Tukey tests were conducted. Both analyses were conducted using PAST 4.03 software [123].

As there were no statistically significant differences in the mean minimum temperature ( $mT_{\min}$ ) between December and January, we did not consider insect collection in December. Fifth instar larvae of *D. rhizophagus* (9.8 mm,  $\pm 1.4$  mm) were collected in the same locality where temperature was recorded, directly from naturally infested Durango pine saplings on 23 November 2022 (November, late fall; during larval migration), 13 January 2023 (January, mid-winter; larvae in the hibernaculum), and 12 February 2023 (February, late winter; larvae preparing pupal chamber). To ensure RNA preservation, the larvae were immediately placed in 1.5 ml-microcentrifuge tubes with 500  $\mu$ l of the RNA stabiliser (RNAlater, Qiagen, Hilden, Germany), puncturing with sterile needle to ensure penetration of the RNA stabiliser, and stored at 4°C until processing before 48 h.

##### 4.2. Total RNA isolation and RNA-Seq

Three biological replicates, one individual per replicate per thermal threshold, were analysed and processed independently. The total RNA of whole larva was extracted using a RiboPure™ RNA purification kit (Ambion® Foster City, CA, USA), according to the manufacturer's protocol. RNA quality and quantity were measured using an Agilent 2100 Bioanalyzer (Agilent Technologies, Santa Clara, CA, USA). Each total RNA sample was used to construct nine cDNA libraries using the TruSeq stranded mRNA kit (Illumina Inc., San Diego, CA, USA) according to the manufacturer's protocol. Sequencing was performed at Macrogen Inc. (Seoul, Korea) using the Illumina NovaSeq 6000 platform (100bp PE).

#### 4.3. Transcriptome assembly

The quality of raw paired-end reads from each library was evaluated using FastQC v.0.11.9 (<https://www.bioinformatics.babraham.ac.uk/projects/fastqc>). Adapter sequences and low-quality reads were removed using Trimmomatic v.0.39 [124] based on a sliding window of kmers = 5, average Phred < 28, and retaining reads > 25 bp. FastUniq v.1.1 [125] and AfterQC v.0.9.7 [126] were used to remove duplicate and poly-X sequences, respectively.

Using default parameters, clean reads from the nine libraries were assembled *de novo* using TRINITY v.2.8 [127]. Transcript redundancies were removed by clustering 95% identity using CD-HIT v.4.8.1 [128]. The transcriptome was assessed based on the percentage of paired reads in the final assembly using Bowtie2 v.2.5.0 [129]. To assess transcriptome completeness, the percentage of orthologous genes was determined in BUSCO v.5.3.1 [130] using the Endopterygota\_odb10 database. The number of full-length transcripts against complete genes from the genome of *D. ponderosae* deposited at the National Center of Biotechnology Information (NCBI) (RefSeq: GCF\_02046658.5.1) was estimated using the Perl script `analyze_blastPlus_topHit_coverge.pl`, as implemented in the TRINITY downstream analysis (<https://github.com/trinityrnaseq/trinityrnaseq/wiki>).

#### 4.4. Differential expression and enrichment analysis

Clean reads from each library were mapped to the *de novo* assembly in Bowtie2 v.2.5.0, to estimate the expression levels of transcripts in RSEM v.1.3.3 [131]. The Trimmed Mean of M-values (TMM) method was used to normalise the transcript abundance matrix of the isoforms. Before differential expression analysis, PCA was carried out with the biological replicates of each thermal threshold to assess the homogeneity among samples using the PtR script included in the TRINITY downstream analysis (<https://github.com/trinityrnaseq/trinityrnaseq/wiki>). To remove PCA outliers, we applied the criteria 2- standard deviation rule estimated from the sample to sample mean distances. Differentially expressed genes (DEGs) were identified at the three thermal thresholds with a Negative Binomial (NB) generalised linear model (GLM), considering a log<sub>2</sub> fold change (log<sub>2</sub>FC) ≥ 2 and false discovery rate (FDR) < 0.01, using the Benjamini-Hochberg method in the edgeR v.4.0.1 package [132] in R software v. 4.3.1. software (R Core Team, 2023).

The open reading frames (ORFs) of the DEGs predicted using TransDecoder v.5.5.0. were annotated by homology searching with BLASTx and BLASTp in NCBI-blast+ v.2.12 using an e-value cut-off ≤ 10<sup>-5</sup> against the Swissprot-Uniprot database [133]. The annotation report was obtained using TRINOTATE v.3.2.2 [133], gene ontology (GO) terms were assigned from the annotation report using TRINOTATE-R (<https://github.com/cstubben/trinotateR>), and metabolic pathways from the Kyoto Encyclopedia of Genes and Genomes (KEGG) from the ORFs were assigned using GhostKOALA tool in the KEGG server (<https://www.kegg.jp/ghostkoala/>) (data not shown) [134].

For each thermal threshold, enrichment analysis of GO terms and KEGG pathways was conducted using the clusterProfiler v.4.8.2 package [135] in R v.4.3.1, considering only the upregulated genes from DEGs previously obtained from the pairwise comparison: late fall vs. mid-winter, mid-winter vs. late winter, late winter vs. late fall. Statistical correction of p-values and FDR was performed using the Benjamini and Hochberg test [136]. Only GO terms and KEGG pathways with p-values < 0.05 and q-values < 0.05, respectively, were considered significant. Lastly,

redundant GO terms were removed using REVIGO server (<http://revigo.irb.hr/>) [137].

#### 4.5. Co-expression networks and Hub-Gene Screening analysis

From the TMM matrix generated with RSEM v.1.3.3 (see section 2.5), gene co-expression networks were built with BioNERO v.1.8.5 package in R v.4.3.1 [137]. Isoforms with average values < 10 were removed from the dataset. The remaining isoforms were then filtered based on their variance values, and only the top 1000 variables were retained. In each network, the standardised connectivity (Z.K.) method was employed to identify outliers and prevent false-positive correlations between a given node and other nodes [139].

Co-expression networks were evaluated using the weighted gene co-expression network analysis (WGCNA) algorithm implemented in BioNERO v.1.8.5 [138]. To find the most suitable  $\beta$  power value to satisfy the scale-free topology, and make the module detection accurate, a default  $\beta$  power value was calculated based on an  $r^2$  threshold > 0.8. The module detection was carried out with a  $\beta$  power value = 5 ( $r^2 = 0.86$ ). To avoid type II errors and evaluate module stability (module persistence across runs), 30 resamples without replacement were performed. For each thermal threshold, negative or positive correlations among gene expressions were calculated using Pearson's correlation test with a  $p$ -value of 0.05. To identify the main functions and metabolic pathways represented at each thermal threshold, an enrichment analysis was performed using clusterProfiler v.4.8.2. Additionally, hub genes (genes with multiple correlations with other genes) were identified by considering the top 10% of the genes with a value > 0.8, module membership (*e.g.* the correlation of a gene with respect to other genes of its own module), and membership degree (*e.g.* the sum of connection weights of a gene with respect to other genes of its own module). Finally, to obtain co-expression networks, subgraph edges (gene-gene interaction weights) were extracted per module and filtered using a correlation threshold value ( $r^2 > 0.7$ ) to eliminate weak correlations among the members of the network.

## References

1. Danks, H. V. The elements of seasonal adaptations in insects. *Can. Entomol.* 139 (1), 1-44 (2007).
2. Dillon, M. E. & Lozier, J. D. Adaptation to the abiotic environment in insects: The influence of variability on ecophysiology and evolutionary genomics. *Curr. Opin. Insect Sci.* 36, 131-139 (2019).
3. Bryant, E. H. A system favoring the holometabolous development. *Ann. Entomol. Soc. Am.* 62 (5), 1087-1091 (1969).
4. Yang, A. S. Modularity, evolvability, and adaptive radiations: a comparison of the hemi- and holometabolous insects. *Evol. Dev.* 3 (2), 59-72 (2001).
5. English, S. & Barreaux, A. M. G. The evolution of sensitive periods in development: insights from insects. *Curr. Opin. Behav. Sci.* 36, 71-78 (2020).
6. Nestel, D. et al. Resource allocation and compensation during development in holometabolous insects. *J. Insect Physiol.* 95, 78-88 (2016).

7. Kostal, V. Insect photoperiodic calendar and circadian clock: independence, cooperation, or unity? *J. Insect Physiol.* 57 (5), 538-556 (2011).
8. Block, et al. Cold tolerance of insects and other arthropods [and discussion]. *Phil. Trans. R. Soc. Lond B.* 326, 613-633 (1990).
9. Lee, R. E. A primer on insect cold tolerance in *Low temperature biology of insects* (ed. Denlinger, D. L., and Lee, R. E.) 3-34 (Cambridge university press, 2010).
10. Bale, J. S. Classes of cold hardiness. *Func. Ecol.* 7, 751-753 (1993).
11. Bale, J. S. Insect cold hardiness: A matter of life and death. *Eur. J. Entomol.* 93, 369-382 (1996).
12. Sinclair, B. J., Vernon, P., Klok, C. J. & Chown S. L. Insects at low temperatures: an ecological perspective. *Trend Ecol. Evol.* 18, 257-262 (2003).
13. Brown, C. L., Bale, J. S. & Walters, K. F. A. Freezing induces a loss of freeze tolerance in an overwintering insect. *Proc. R. Soc. Lond. B.* 271, 1507-1511 (2004).
14. Lombardero, M. J., Ayres, M. P., Ayres, B. D. & Reeve, J. D. Cold tolerance of four species of bark beetle (Coleoptera: Scolytidae) in North America. *Environ. Entomol.* 29 (3), 421-432 (2000).
15. Dennis, A. B., Dunning, L. T, Dennis, C. J., Sinclair, B. J. & Buckley T. R. Overwintering in New Zealand stick insects. *N. Z. Entomol.* 37 (1), 35-44. (2014).
16. Wang, J., Zeng L. & Han, Z. An assessment of cold hardiness and biochemical adaptation for cold tolerance among different geographic populations of the *Batrocera dorsalis* (Diptera: Tephritidae) in Cina. *J. Insect Sci.* 14 (292), 1-6 (2014).
17. Fernández, D. C., VanLaerhoven, S. L., Sinclair B. J. & Labbé, R. M. Effects of acclimation on the cold tolerance of the pepper weevil. *J. Pest. Sci.* 1-11 (2025).
18. Victor, J. & Zúñiga, G. Phylogeny of *Dendroctonus* bark beetles (Coleoptera: Curculionidae: Scolytinae) inferred from morphological and molecular data. *Syst. Entomol.* 41 (1), 162-177 (2015).
19. Valerio-Mendoza, O. et al. Cryptic species discrimination in western pine beetle, *Dendroctonus brevicomis* LeConte (Curculionidae: Scolytinae), based on morphological characters and geometric morphometrics. *Insects.* 10, 377 (2019).

20. Smith, R. H. Red turpentine beetle. (Department of Agriculture), Forest Service. *Forest and Insect Disease leaflet*. 55, 1-9 (1971).
21. Schebeck, M. et al. Diapause and overwintering of two spruce bark beetle species. *Physiol. Entomol.* 42 (3), 200-210 (2017).
22. Robert, J. A. et al. Gene expression analysis of overwintering mountain pine beetle larvae suggests multiple systems involved in overwintering stress, cold hardiness and preparation for spring development. *PeerJ.* 4, e2109 (2016).
23. Bleiker, K. P. & Smith, G. D. Cold tolerance of mountain pine beetle (Coleoptera: Curculionidae) pupae. *Physiol. Ecol.* 48 (6), 1412-1417 (2019).
24. Bonnett, T. R. et al. Global and comparative proteomic profiling of overwintering and developing mountain pine beetle, *Dendroctonus ponderosae* (Coleoptera: Curculionidae), larvae. *Insect Biochem. Mol. Biol.* 42 (12), 890-901 (2012).
25. Fu, D. et al. Effects of cold stress on metabolic regulation in the overwintering larvae of the Chinese white pine beetle, *Dendroctonus armandi*. *Entomol. Exp. Appl.* 168 (11), 836-850 (2020).
26. Thomson, K. M., Huber, D. P. W. & Murray, B. W. Autumn shifts in cold tolerance metabolites in overwintering adult mountain pine beetles. *PLoS one.* 15 (1), e0227203 (2020).
27. Fraser, J. D., Bonnet, T. R., Keeling, C. I. & Huber, D. P. W. Seasonal shifts in accumulation of glycerol biosynthetic gene transcripts in mountain pine beetle, *Dendroctonus ponderosae* Hopkins (Coleoptera: Curculionidae), larvae. *PeerJ.* 5, e3284 (2017).
28. Zhao, D. et al. Expression analysis of genes related to cold tolerance in *Dendroctonus valens*. *PeerJ.* 9, e10864 (2021).
29. Wang, J., Gao, G., Zhang, R., Dai, L. & Chen, H. Metabolism and cold tolerance of Chinese white pine beetle *Dendroctonus armandi* (Coleoptera: Curculionidae: Scolytinae) during the overwintering period. *Agric. For. Entomol.* 19 (1), 10-22 (2017).

30. Yan, Z., Sun, J., Don, O. & Zhang, Z. The red turpentine beetle, *Dendroctonus valens* LeConte (Scolytidae): an exotic invasive pest of pine in China. *Biodivers. Conserv.* 14, 1735-1760 (2005).
31. Wang, J., Zhang, R. R., Gao, G. Q., Ma, M. Y. & Chen H. Cold tolerance and silencing of three cold-tolerance genes of overwintering Chinese white pine larvae. *Sci. Rep.* 6(34698), 1-17 (2016)
32. Fu, D., Sun, Y., Gao, H., Liu, B., Kang, X. & Chen H. Identification and functional characterization of antifreeze protein and its mutants in *Dendroctonus armandi* (Coleoptera: Curculionidae: Scolytinae) larvae under cold stress. *Physiol. Ecol.* 51(1), 167-181 (2022).
33. Régnière, J. & Bentz, B. Modeling cold tolerance in the mountain pine beetle, *Dendroctonus ponderosae*. *J. Insect Physiol.* 53, 559-572 (2007).
34. Lester, J. D. & Irwin, J. T. Metabolism and cold tolerance of overwintering adult mountain pine beetles (*Dendroctonus ponderosae*): evidence of facultative diapause? *J. Insect Physiol.* 58 (6), 808-815 (2012).
35. Ungerer, M. J., Ayres M. P. & Lombardero, M. J. Climate and northern distribution limits of *Dendroctonus frontalis* Zimmermann (Coleoptera: Scolytidae). *Journal of Biogeography.* 26(1), 1133-1145 (2003).
36. Dodds, K., J., et al. Expansion of southern pine beetle into northeastern forest: management and impact of primary bark beetle in a new region. *J. For.* 116(2), 178-191 (2018).
37. Thomas, J. B., & Bright Jr., D. E. A new species of *Dendroctonus* (Coleoptera: Scolytidae) from Mexico. *Can. Entomol.* 102 (4), 479-483 (1970).
38. Kyre, B. R. & Rieske, L. K. Using RNAi to silence heat shock protein has congeneric effects in North America's *Dendroctonus* bark beetles. *For. Ecol. Manag.* 520, 1-8 (2022).
39. Kyre, B. R., Dupuis, J. R., Zúñiga, G. & Rieske L. K. Variation in RNA interference sensitivity in the southern pine beetle, *Dendroctonus frontalis* (Coleoptera: Curculionidae). *Biol. J. Linn. Soc.* 142, 147-154 (2024).

40. Christiaens, O., Sweet, J., Dzhambazova, T., Urru, I., Smagghe, G., Kostov, K. & Arpaia, S. Implementation of RNAi-based arthropod pest control: environmental risks, potential for resistance and regulatory considerations. *J. Pest. Sci.* 95(1), 1-15 (2022).
41. Hoshikawa, K., Tsutsui, H., Honma, K. & Sakagami, S. F. Cld resistance in four species of beetle overwintering in the soil, with notes in overwintering strategies of some soil insects. *Appl. Ent. Zool.* 23(3), 273-281 (1988).
42. Jian, F., Jayas, D. S. & White, N. D. G. Movement of adult rusty grain beetles, *Cryptolestes ferrugineus* (Coleoptera: Cucujidae), in wheat in response to 5°/m temperature gradients at cool temperatures. *J. Stored. Prod. Res.* 39, 87-101 (2003).
43. Yamazaki, K., Sugiura, S. & Kawamura, K. Ground beetles (Coleoptera: Carabidae) and other insect predators overwintering in arable and fallow field in central Japan. *Appl. Entomol. Zool.* 38(4), 449-459 (2003).
44. Nalepa, C. A., Kennedy, G. G. & Brown, C. Role of visual contrast in the alighting behavior of *Harmonia axyridis* (Coleoptera: Coccinellidae) at overwintering sites. *Environ. Entomol.* 34(2) 425-431 (2005).
45. Roach, S. H. Natural plant materials as overwintering sites for arthropods in the coastal plain of South Carolina. *Fla. Entomol.* 74(4), 543-554 (1991).
46. Bennett, V. A., Lee, R. E., Nauman, J. S. & Kukal O. Selection of overwintering microhabitats used by the arctic woollybear caterpillar, *Gynaephora groenlandica*. *CryoLett.* 24, 191-200 (2003).
47. Brodeur, J. & McNeil J. M. Overwintering microhabitat selection by an endoparasitoid (Hymenoptera: Aphididae): Induced phototactic and thigmokinetic responses in dying host. *J. Insect Behav.* 3(6), 751-762 (1990).
48. Tanaka, S. Temperature-dependent phototaxis in overwintering adults of the *Patanga japonica* (Orthoptera, Acrididae). *J. Orthoptera Res.* 33(1), 71-86 (2004).
49. He, H., Zhao, R., Hu, K., Qiu, L., Ding, W. & Li, Y. A novel negative thermotaxis behavior in rice planthoppers is regulated by TRPA1 channel. *Pest Manag. Sci.* 76(9), 3003-3011 (2020).

50. Hodek, I. Bionomic and ecology of predaceous Coccinellidae. *Ann. Rev. Entomol.* 12 79-104 (1967).
51. Akers, R. P. Counterturns initiated by decrease in rate of increase of concentration: Possible mechanism of chemotaxis by walking female *Ips paraconfusus* bark beetles. *J. Chem. Ecol.* 15(1), 183-208 (1989).
52. Bellemer, A. Thermotaxis, circadian rhythms, and TRP channels in *Drosophila*. *Temperature.* 2(2), 277-243 (2015).
53. Yuichiro, O. & Korsching, S. I. The fifth element in animal  $\alpha$  protein evolution. *Commun. Integr. Bio.* 2 (3), 227-229 (2009).
54. Luo, L. et al. Navigational decision making in *Drosophila* Thermotaxis. *J. Neurosci.* 30(12), 4261-4272 (2010).
55. Rosenzweig, M., Kang, K. & Garrity, P. A. Distinct TRP channels are required for warm and cold avoidance in *Drosophila melanogaster*. *PNAS.* 105(38), 14668-14673 (2008).
56. Gong, J. et al. A cold sensing receptor encoded by a glutamate receptor gene. *Cell.* 178, 1375-1386 (2019).
57. Johnson, B. R., Atallah, J. & Plachetzki, D. C. The importance of tissue specificity for RNA-seq: Highlighting the errors of composite structure extractions. *BMC Genomics.* 14(586), 1471-2164 (2013).
58. Deneubourg, J. L., Grégoire, J. C. & Le, F. E. Kinetics of larval gregarious in the behavior in the bark beetle *Dendroctonus micans* (Coleoptera: Scolytidae). *J. Insect Behav.* 3, 169-182 (1990).
59. Furniss, M. M. Biology of *Dendroctonus punctatus* (Coleoptera: Scolytidae). *Ann. Entomol. Soc. Am.* 88(2), 173-182 (1995).
60. Zhu, J. et al. General odorant-binding proteins and sex pheromone guide larvae of *Plutella xylostella* to better food. *Insect Biochem. Mol. Biol.* 72: 10-19 (2016).
61. Hao, E. et al. Key residues affecting binding affinity of *Sirex noctilio* Fabricius odorant-binding protein (SnocOBP9) to aggregation pheromone. *Int. J. Mol. Sci.* 23 (8456), 1-25 (2022).

62. Andersson, M. N. et al. 2013. Antennal transcriptome analysis of the chemosensory gene families in the tree killing bark beetles, *Ips typographus* and *Dendroctonus ponderosae* (Coleoptera: Curculionidae: Scolytinae). *BMC Genomics*. 14(198), 1471-2164 (2013).
63. Rihani, K., Ferveur, J. F. & Briand, L. The 40-year mystery of insect odorant binding proteins. *Biomolecules*. 11(509), 1-27 (2021).
64. Hertzog, W., Powers, K., Johnston, K. & Duvall, M. A new paradigm for muscle contraction. *Front. Physiol.* 2015. 6(174) (2015).
65. Schöck, F. & González-Morales, N. The insect perspective on Z-disc structure and biology. *J. Cell Sci.* 135 (20), jcs260179 (2022).
66. Ashraf, M. Z. et al. Comparative gut proteomics study revealing adaptive physiology of Eurasian spruce bark beetle, *Ips typographus* (Coleoptera: Scolytinae). *Front. Plant Sci.* 14(1157455), 1-21 (2023).
67. Nasser, A., Mogilicherla, K., Sellamuthu, G. & Roy A. Age matters: Life-stage, tissue, and sex-specific gene expression dynamics in *Ips typographus* (Coleoptera: Curculionidae: Scolytinae). *Front. For. Glob. Change.* 6(1124754), 1-26 (2023).
68. Eyun, S. et al. Molecular evolution of glycoside hydrolase genes in the western corn rootworm (*Diabrotica virgifera virgifera*). *PLoS one.* 9 (4), e94052 (2014).
69. Panevska, A., Skočaj, M., Križaj, I., Maček, P. & Sepčić, K. Ceramide phosphoethanolamine, an enigmatic cellular membrane sphingolipid. *Biomembranes*. 1861, 1284-1292 (2019).
70. Vukašinović, E. L. et al. Diapause induces remodeling of the fatty acid composition of membrane and storage lipids in overwintering larvae of *Ostrinia nubilalis*, Hubn. (Lepidoptera: Crambidae). *Comp. Biochem. Physiol. B. Biochem. Mol. Biol.* 184: 36-43 (2015).
71. Trenti, F., Sandron, T., Guella, G. & Lencioni, V. Insect cold-tolerance and lipodome: membrane lipid composition of two chironomid species differently adapted to cold. *Cryobiology*. 106, 84-90 (2022).

72. Sinclair, B. J. & Marshall, K. E. The many roles of fats in overwintering Insects. *J. Exp. Biol.* 221(Suppl\_1), 1-9 (2018).
73. Rothblat, G. H., Mahlberg, F. H., Johnson, W. J. & Phillips, M. C. Alipoproteins, membrane cholesterol domains, and the regulation of cholesterol efflux. *JLR.* 33 (8), 1091-1097 (1992).
74. Gillotte, K. L. et al. Apolipoprotein-mediated plasma membrane microsolubilization role of lipid affinity and membrane penetration in the efflux of cellular cholesterol and phospholipid. *Cell Metab.* 274 (4), 2021-2028 (1999).
75. Parker, D. J., Ritchie, M. G. & Kankare, M. Preparing for winter: the transcriptome response associated with different day lengths in *Drosophila montana*. *G3: Genes/Genomes/Genetics.* 6 (5), 1373-1381 (2016).
76. Bayley, J. S., Sorensen, J. G., Moos, M., Kostal, V. & Overgaard, J. Cold acclimation increases depolarization resistance and tolerance in muscle fibers from a chill-susceptible insect, *Locusta migratoria*. *Am. J. Physiol. Regul. Integr. Comp. Physiol.* 319 (4), R439-R447 (2020).
77. Wang, X., Yu, H., Gao, R., Liu, M. & Xie, W. A comprehensive review of the family of very-long-chain fatty acid elongases: structure, function and implications in physiology and pathology. *Eur. J. Med. Res.* 28 (532), (2023).
78. Kayukawa, T., Chen, B., Hoshizaki, S. & Ishikawa, Y. Upregulation of a desaturase is associated with the enhancement of cold hardiness in the onion maggot, *Delia antiqua*. *Insect Biochem. Mol. Biol.* 37, 1160-1167 (2007).
79. Lev, S. Nonvesicular lipid transfer from endoplasmic reticulum. *Cold Spring Harb. Perspect. Biol.* 4(10), a013300 (2012).
80. Wigger, D., Gulbins, E., Kleuser, B. & Schumacher, F. Monitoring the sphingolipid de novo synthesis by stable-isotope labeling and liquid chromatography mass spectrometry. *Front. Cell Dev. Biol.* 7, 210 (2019).
81. Rozsypal J., Kostal, V., Berkova, P., Zahradnickova H. & Simek, P. Seasonal changes in the composition of storage and membrane lipids in overwintering larvae of the codling moth, *Cydia pomonella*. *J. Therm. Biol.* 45, 124-133 (2014).

82. Govaere, L. et al. Transcriptome and proteome analyses to investigate the molecular underpinnings of cold response in the Colorado potato beetle, *Leptinotarsa decemlineata*. *Cryobiology*. 88, 54-63 (2019).
83. Bartke, N. & Hannun, Y. A. Bioactive sphingolipids: metabolism and function. *JLR*. 50, S91-S96 (2008).
84. Toprak, U., Hegedus, D., Dogan, C. & Güney, G. A journey into the world of insect lipid metabolism. *Insect Biochem. Physiol.* 104, e21682 (2020).
85. Skowronek, P., Wójcik, L. & Strachecka A. Fat-boby-Multifunctional Inset Tissue. *Insects*. 12(547), 1-25 (2021).
86. He, A., Dean, J. M. & Lodhi, I. J. Peroxisomes as cellular adaptors to metabolic and environmental stress. *Trends Cell Biol.* 31(8), 656-670 (2021).
87. da Silva, R. M. et al. PRPCK and glucose metabolism homeostasis in arthropods. *Insect. Biochem. Mol. Biol.* 160, 103986 (2023).
88. Spacht, D. E., Teets, N. M. & Denlinger, D. L. Two isoforms of PEPCCK in *Sarchophaga bullata* and their distinct expression profiles through development, diapause and in response to stresses of cold and starvation. *J. Insect Physiol.* 111, 41-46 (2018).
89. Olsson, T. et al. Hemolymph metabolites and osmolality are tightly linked to cold tolerance of *Drosophila* species: A comparative study. *J. Exp. Biol.* 29 (16), 2504-2513 (2016).
90. Teets, N. M, Kawarasaki, Y., Lee, R. E. & Denlinger, D. L. Expression of genes involved in energy mobilization and osmoprotectant synthesis during thermal and dehydration stress in the Antarctic midge, *Belgica antarctica*. *J. Comp. Physiol. B.* 183, 189-201 (2013).
91. Hahn, D. A. & Denlinger, D. L. Energetics of insect diapause. *Annu. Rev. Entomol.* 56, 103-121 (2011).
92. Lan, T. et al. Transcriptome and expression analysis of glycerol biosynthesis-related genes in *Glanea cantor* Fabricius (Cerambycidae: Lamiinae). *In. J. Mol. Sci.* 25(11834), 1-15 (2024).

93. Feder, M. E. Heat shock proteins, molecular chaperons, and the stress response: Evolutionary and ecological physiology. *Annu. Rev. Physiol.* 61, 243-282 (1999)
94. Banfi, D., Bianchi, T., Mastore, M. & Brivio M. F. The role of heat shock proteins in stress response, immunity, and climate adaptation. *Insects.* 16(741), 1-11 (2025).
95. Wronska, A. K. & Bogus, M. I. Heat shock proteins (HSP 90, 70, 60 and 27) in *Galleria mellonella* (Lepidoptera) hemolymph are affected by infection with *Conidiobolus coronatus* (Entomophthorales). *PLoS one.* 15 (2), e0228556 (2020).
96. Jang, S. et al. Dual oxidase enables insect gut symbiosis by mediating respiratory network formation. *Proc. Natl. Acad. Sci. USA.* 118 (10), e2020922118 (2021).
97. Bai S., Yaou, Z., Raza, M. F., Cai, Z. & Zhang, H. Regulatory mechanism of microbial homeostasis in insect gut. *Insect Sci.* 28 (2), 286-301 (2021).
98. Ha, E., Oh, C., Bae, Y. S. & Lee, W. A direct role for dual oxidase in *Drosophila* gut immunity. *Science.* 310 (5749), 847-850 (2005).
99. Yao, Z., Wang A., Li, Y., Cai, Z., Lemaitre, B. & Zhang, H. The dual oxidase gene *BdDuoX* regulates the intestinal bacterial community homeostasis of *Bactrocera dorsalis*. *The ISME J.* 10 (5), 1037-1050 (2016).
100. Donkó, Á., Péterfi, Z., Sum, A., Leto, T. & Geiszt, M. Dual oxidases. *Philos. Trans. R. Soc. B.* 360 (1464), 2301-2308 (2005).
101. Nielsen, M. M. et al. Role of HSF activation for resistance to heat, cold and high-temperature knock-down. *J. Insect Physiol.* 51 (12), 1320-1329 (2005).
102. Königer, A. & Grath, S. Transcriptome analysis reveals candidate genes for cold tolerance in *Drosophila ananassae*. *Genes.* 9 (12), 624 (2018).
103. Lalouette, L., Williams, C. M., Hervant, F., Sinclair, B. J. & Renault, D. Metabolic rate and oxidative stress in insects exposed to low temperatures thermal fluctuations. *Comp. Biochem. Physiol. A Mol. Integr. Physiol.* 158 (2), 229-234 (2011).
104. Pham, D. Q. D. & Winzerling, J. J. Insect ferritins: typical or atypical? *Biochim. Biophys. Acta - Gen. Subj.* 1800 (8), 824-833 (2010).

105. Abbas, M. N. et al. Molecular characterization. immune functions and DNA protective effects of Peroxiredoxin-1 gene in *Antheraea pernyi*. *Mol. Immunol.* 170, 76-87 (2024).
106. Qu, J., Zou, T. & Lin, Z. The roles of the ubiquitin-proteasome system in the endoplasmic reticulum stress pathway. *Int. J. Mol. Sci.* 22 (4), 1526 (2021).
107. Sasibhushan, S., Ponnuvel, K. M. & Vijayaprakash, N. B. Diapause specific gene expression in the eggs of multivoltine silkworm *Bombix mori*, identified by suppressive subtractive hybridization. *Comp. Biochem. Physiol. B Biochem. Mol. Biol.* 161(4), 371-379 (2012).
108. Pei, J., Xu, Y., Zong, S. & Ren, L. Transcriptome and metabolomic data reveal the key metabolic pathways affecting *Streltzoviella insularis* (Staudinger) (Lepidoptera: Cossidae) larvae during overwintering. *Front. Physiol.* 12, 655059 (2021).
109. Clister, T., Mehta, S. & Zhang, J. Single-cell analysis of G-protein signal transduction. *J. Biol. Chem.* 290 (11), 6681-6683 (2015).
110. Xia, H. J. & Yang, G. Inositol 1,4,5-triphosphate 3-kinases: functions and regulations. *Cell Res.* 15 (2), 83-91 (2005).
111. Lin, Y., Seroude, L. & Benzer, S. Extended-life span and stress resistance in the *Drosophila* mutant *Methuselah*. *Science.* 282 (5390), 943-946 (1998).
112. Li, Y. et al. Characterization and expression profiling of G protein-coupled receptors (GPCRs) in *Spodoptera litura* (Lepidoptera: Noctuidae). *Comp. Biochem. Physiol. Part D Genomics Proteomics.* 44, 101018 (2022).
113. Keeling, C. I. et al. CYP345E2, an antenna-specific cytochrome P450 from the mountain pine beetle, *Dendroctonus ponderosae* Hopkins, catalyzes the oxidation of pine host monoterpene volatiles. *Insect Biochem. Mol. Biol.* 43 (12), 1142-1151 (2013).
114. Sarabia, L. E. et al. Time-course of CYP450 gene expression from *Dendroctonus rhizophagus* (Curculionidae: Scolytinae) during early hours of drilling bark and settling into the host tree. *J. Insect Sci.* 19 (3), 11 (2019).

115. Torres-Banda, V. et al. Gut transcriptome of two bark beetle species stimulated with the same kairomones reveals molecular differences in detoxification pathways. *Comput. Struct. Biotechnol. J.* 20, 3080-3095 (2022).
116. Quijano-Barraza, J. M. et al. Evolution and functional role of the CYP6DE and CYP6DJ subfamilies in *Dendroctonus* (Curculionidae: Scolytinae) bark beetles. *Front. Mol. Biosci.* 10, 1274838 (2023).
117. McBrayer, Z., et al. Prothoracicotropic hormone regulates developmental timing and body size in *Drosophila*. *Dev. Cell.* 13, 857-871 (2007).
118. Hodek, I. Dormancy in *Ecology of Coccinellidae* (ed. Hodek, I. & Honěk, A.) 239-318 (Springer Dordrecht).
119. Hahn, D. A. & Denlinger, D. L. Energetics of insect diapause. *Annu. Rev. Entomol.* 56, 103-121 (2011).
120. Consoulas, C., Duch, C., Bayline, R. J. & Levine, R. B. Behavioral transformations during metamorphosis: remodeling of neural and motor systems. *Brain Res. Bull.* 53 (5), 571-583 (2000).
121. Katzemich, A. et al. Binding partners of the kinase domains in *Drosophila* obscurin and their effect on the structure of flight muscle. *J. Cell Sci.* 128, 3386-3397 (2015).
122. Six, D. L. & Klepzig, K. D. *Dendroctonus* bark beetles as model systems for studies on symbiosis. *Symbiosis.* 37, 1-27 (2004).
123. Hammer, O., Harper, D. A. T. & Ryan, P. D. PAST: Paleontological Statistics software package for education and data analysis. *Palaeontol. Electron.* 4 (1), 1-9 (2001).
124. Bolger, A. M., Lohse, M. & Usadel, B. Trimmomatic: A flexible trimmer for Illumina sequence data. *Bioinformatics.* 30 (15), 2114-2120 (2014).
125. Xu, H. et al. FastUniq: A fast de novo duplicates removal tool for paired short reads. *Plos one.* 7 (12), e52249 (2012).
126. Chen, S. et al. AfterQC: Automatic filtering, trimming, error removing, and quality control for fastq data. *BMC bioinformatics.* 18 (80), 91-100 (2017).

127. Haas, B. J. et al. De *nov*o transcript sequence reconstruction from RNA-seq using the Trinity platform for reference generation and analysis. *Nat. Protoc.* 8 (8), 1494-1512 (2013).
128. Fu, L., Niu, B., Zhu, Z., Wu, S., & Li, W. CD-HIT: Accelerated for clustering the next-generation sequencing data. *Bioinformatics.* 28 (23), 3150-3152 (2012).
129. Langmead, B. & Salzberg, S. Fast gapped-read alignment with Bowtie 2. *Nat. Methods.* 9 (4), 357-359 (2012).
130. Manni, M. et al. M. BUSCO update: novel and streamlined workflows along with broader and deeper phylogenetic coverage for scoring of eukaryotic, prokaryotic, and viral genomes. *Mol. Biol. Evol.* 38 (10), 4647-4654 (2021).
131. Li, B. & Colin, N. D. RSEM: Accurate transcript quantification from RNA-Seq data with or without a reference genome. *BMC bioinformatics.* 4 (12), 323 (2011).
132. Robinson, M. D., McCarthy, D. J. & Smyth, G. K. edgeR: a Bioconductor package for differential expression analysis of digital gene expression data. *Bioinformatics.* 26 (1), 139-140 (2010).
133. Bryant, D. M. et al. A tissue-mapped axolotl de novo transcriptome enables identification of limb regeneration factors. *Cell Rep.* 3 (18), 762-776 (2017).
134. Kanehisa, M. & Goto, S. KEGG: Kyoto Encyclopedia of Genes and Genomes. *Nucleic Acids Res.* 28, 27-30 (2000)
135. Wu, T. et al. ClusterProfiler 4.0: A universal enrichment tool for interpreting omics data. *Innov.* 2 (3), 1-10 (2021).
136. Benjamini, Y., Drai, Dan, Elmer, G., Kafkafi N. & Golani, I. Controlling the false discovery rate in behavior genetics research. *Behav. Brain Res.* 125 (1-2), 279-284 (2001).
137. Supek F., Bošnjak M., Škunca N., & Šmuc T. REVIGO summarizes and visualizes long list of gene ontology terms. *PLoS one.* 6(7): e21800 (2011).
138. Almeida-Silva, F. & Venencio, T. M. BioNERO: an all-in-one R/Bioconductor package from comprehensive and easy biological network reconstruction. *Funct. Integr. Genomics.* 22 (1), 131-136 (2022).

139. Xu, X. et al. Identification of stress-related genes by co-expression network analysis based on the improved turbot genome. *Sci. Data*. 9 (1), 374 (2022).

**Acknowledgments:** We thank to Arnulfo Albores Medina and Héctor Manuel Oliver Hernández for allowing the use of Xicoatl Hybrid Supercomputing Cluster of CINVESTAV-IPN; to Ildelfonso Ceballos Molina, José Gildardo Bustillos Torres, and Hernán Efraín Escalante Olgún from the Región de Manejo Silvícola de Guachochi A. C. for their assistance in collecting larvae; to Rosa María Pineda Mendoza for the figures editing; and three anonymous reviewers for their comments.

**Author Contributions:** Conceptualization, M.B., M.F.L., C.C.R., and G.Z.; Methodology, M.B., V.T.B., and J.M.Q.B.; Software, M.B.; V.T.B., and J.M.Q.B.; Validation, M.B., G.O.M., V.T.B. and G.Z.; Formal Analysis, M.B.; V.T.B., M.F.L., C.C.R., G.O.M, J.M.Q.B., and G.Z.; Investigation, M.B., G.Z; Resources, G.Z.; Data Curation, M.B.; Writing – Original Draft Preparation, M.B.; and G.Z.; Writing – Review & Editing, M.B.; V.T.B., M.F.L., C.C.R., G.O.M, J.M.Q.B., and G.Z.; Visualization, M.B.; Supervision, G.Z.; Project Administration, G.Z.; Funding Acquisition, G.Z. All authors have read and approved the final manuscript.

**Data Availability Statement:** Sequence data that support the findings of this study have been deposited in the National Center of Biotechnology Information (NCBI) with the primary accession code PQ675428-PQ675541 and PV416796- PV416799.

**Funding:** This research was partially funded by Consejo Nacional de Ciencia y Tecnología (CONACyT-CB 2012/181337) and Secretaría de Investigación y Posgrado del IPN (SIP-20221610). This work was part of M.B.'s PhD dissertation, and M.B. (CVU 814034), J.M.Q.B. (CVU 1008241), and V.T.B. (CVU 232939) were fellows of Beca de Estímulo Institucional de Formación de Investigadores (BEIFI-IPN) and the Consejo Nacional de Humanidades, Ciencia y Tecnología (CONAHCYT).

**Declaration of Competing Interest:** The authors declare that they have no known competing financial interests or personal relationships that could have appeared to influence the work reported in this paper.

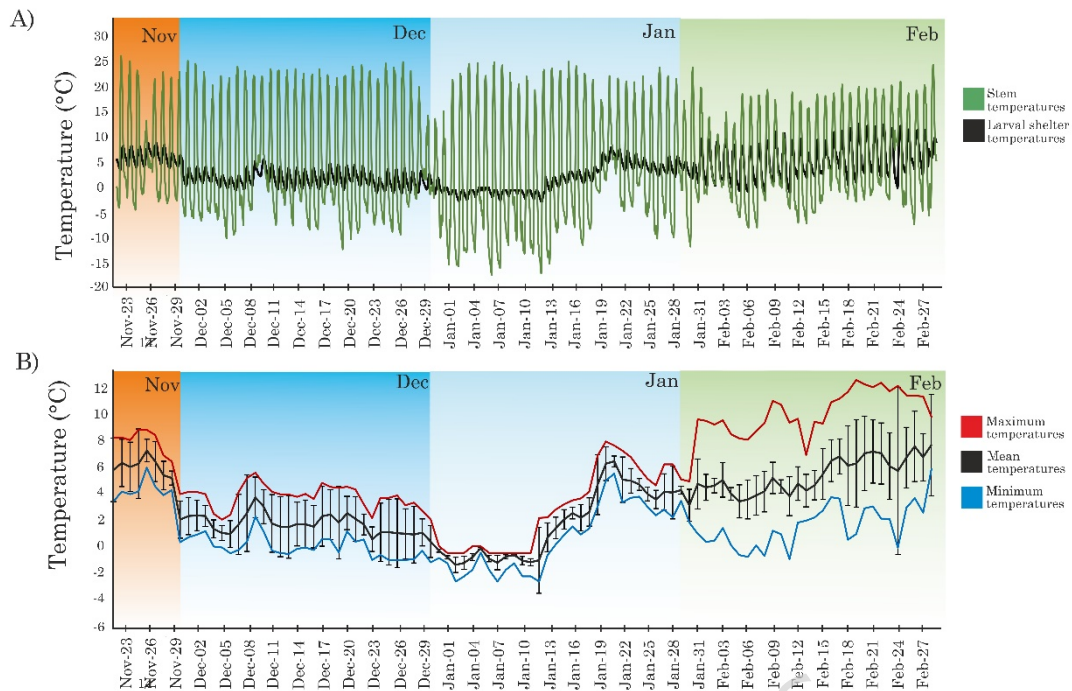


**Figure 1.** Climograms of the mean hourly temperature from November to February in the years 2019-2020, 2020-2021, and 2021-2022 ( $n = 25,920$  temperature records/ microsite (stem and hibernaculum)/ month). A) Temperature oscillation in the sapling stem (green) compared to the larval hibernaculum (black),  $t = 6.45$ ,  $p < 0.001$ . B) Mean (black), maximum (red), and minimum (blue) temperatures and their standard deviation (bars) at larval hibernaculum,  $F = 434.7$ ,  $p < 0.001$ .

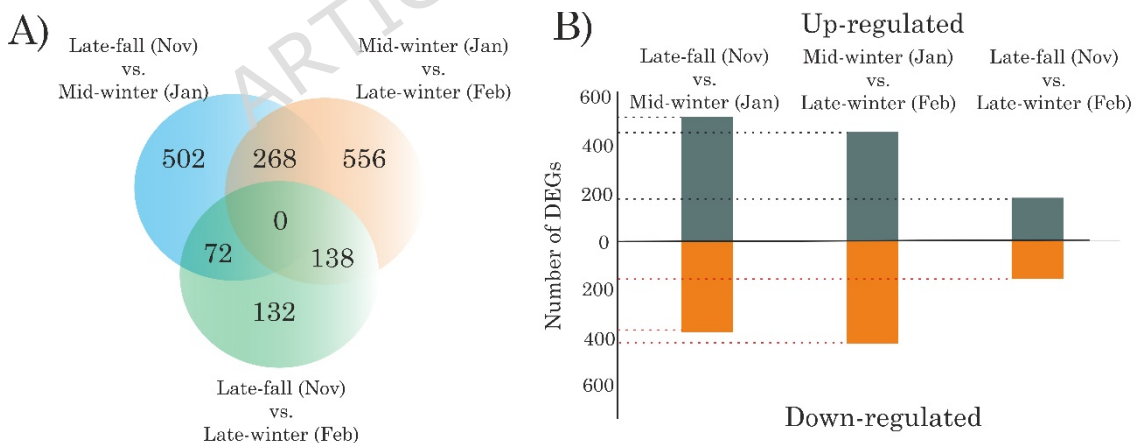


**Figure 2.** Differential expressed genes (DEGs,  $\log_2FC \geq 2$ ,  $FDR < 0.01$ ) in the fifth instar larvae of *D. rhizophagus* during cold season, obtained across the pairwise comparison between the three thermal thresholds: late-fall (Nov), mid-winter (Jan) and late-winter (Feb). A) The Venn diagram shows the exclusive and shared DEGs among the three thermal thresholds. B) Number of up- and down-regulated DEGs among pairwise comparisons.

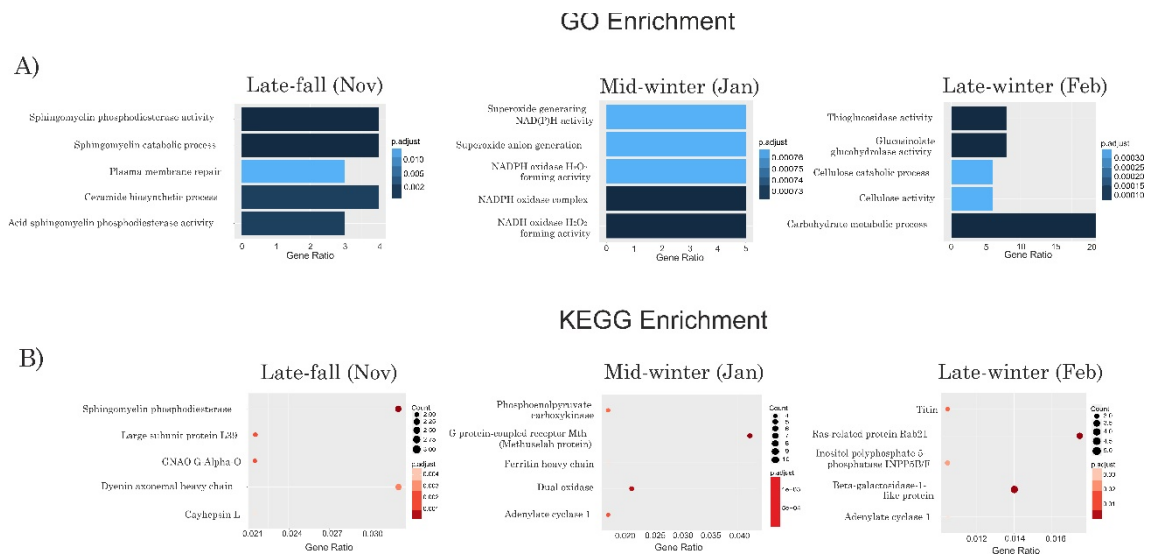


**Figure 3.** Main enriched GO terms and KEGG orthologous groups related to cold hardiness of the fifth instar larvae of *D. rhizophagus* during three thermal thresholds: late-fall (Nov), mid-winter (Jan), and late-winter (Feb). A) Ratio of GO enriched terms related to cellular membrane in late-fall, oxidative stress in mid-winter, and carbohydrate metabolism in late-winter. B) Ratio of KEGG enriched orthologous groups related to cellular membrane and signal transduction in late-fall, oxidative stress and energy metabolism in mid-winter, and signaling and muscular activity in late-winter. Color scales represent  $p$  values  $< 0.05$ , bar and circle sizes represent the genes ratio in GO terms and KEGG orthologous groups, respectively.

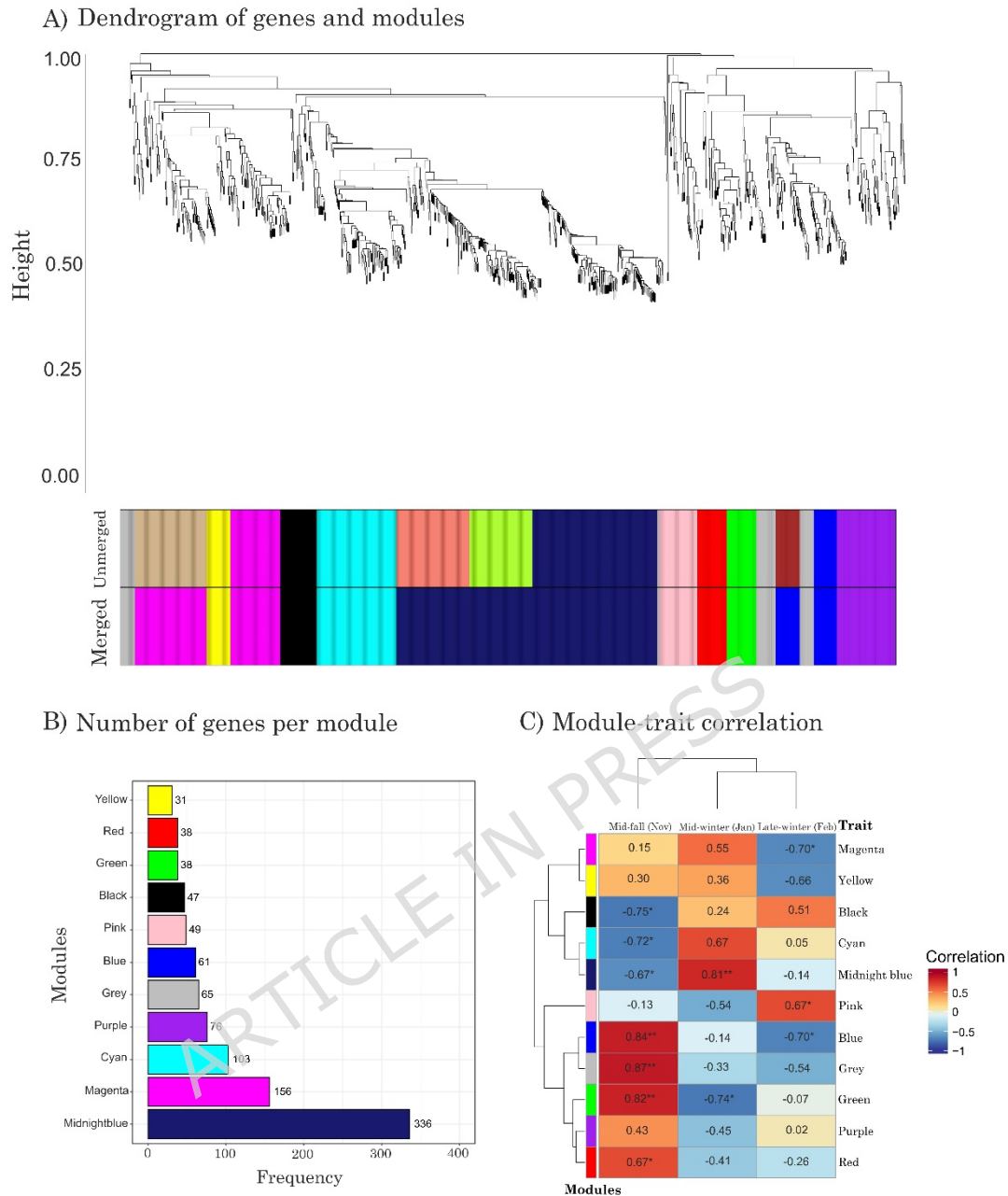


**Figure 4.** Co-expression analysis of the transcriptome of *D. rhizophagus* fifth instar larvae during the thermal thresholds: late-fall (Nov), mid-winter (Jan), and late-winter (Feb). A) Co-expressed gene modules identified from gene clustering analysis (dendrogram) based on the estimated  $\beta$  power value. B) Number of genes per module. C) Positive and negative Pearson's correlation values of co-expressed genes within each module per thermal threshold. Significant correlations are shown in the boxes with  $p$ -value  $< 0.05$  "\*", and  $p$ -value  $< 0.005$  "\*\*".

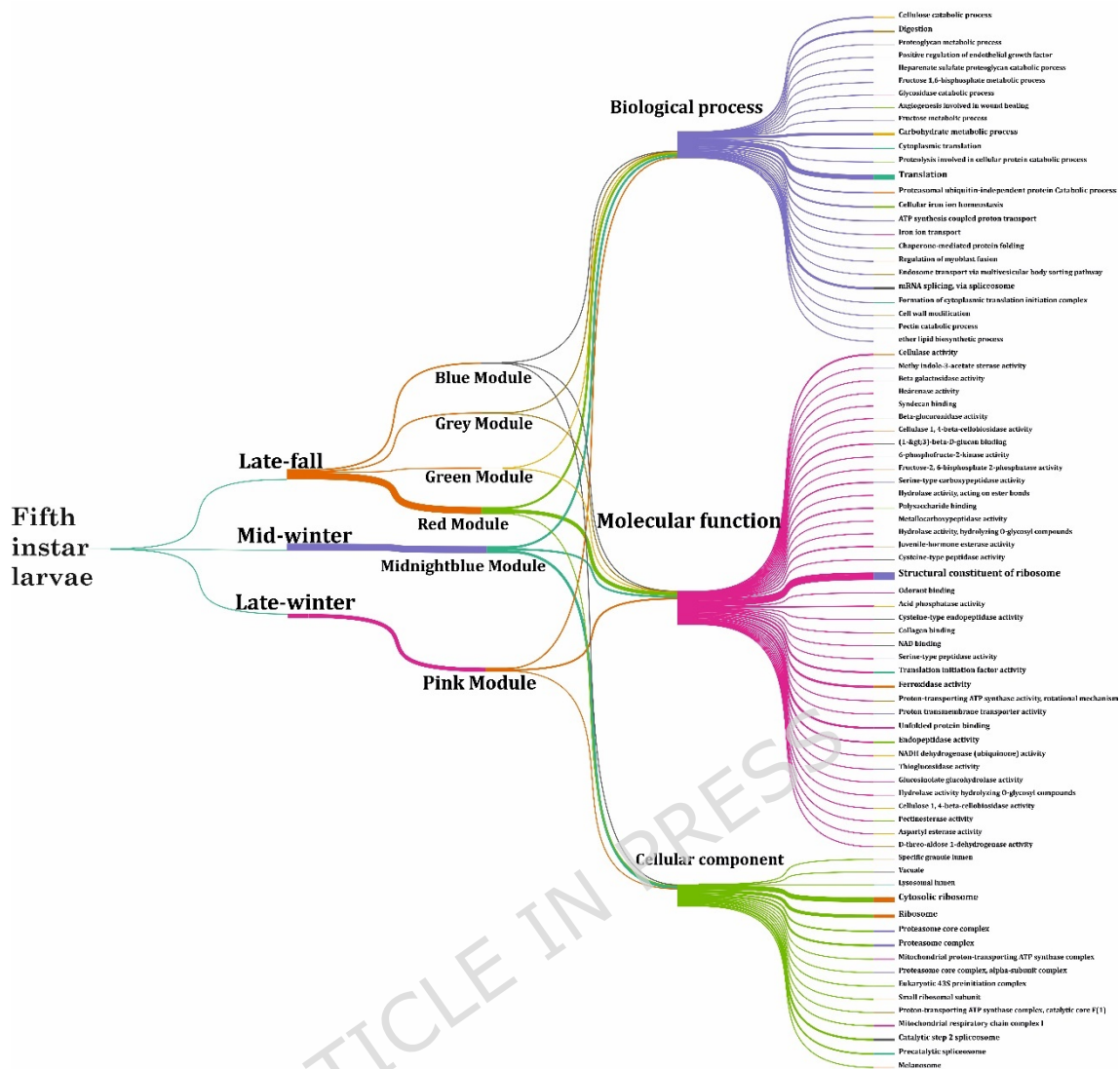


**Figure 5.** The Sankey diagram illustrates the associations between co-expressed gene modules detected across seasonal stages (late-fall, mid-winter, and late-winter) and the main Gene Ontology (GO) categories: Biological Process, Molecular Function, and Cellular Component. Each module (e.g., Pink, Midnightblue, Red, Green, Grey, and Blue) represents a cluster of genes with highly correlated expression patterns. The connections depict the relative contribution of each module to representative biological functions, highlighting processes related to translation, ribosomal assembly, energy metabolism, and seasonal stress response.

**Table 1.** ANOVA and Tukey’s post hoc test of mean temperatures recorded in the hibernaculum from November to February of the years 2019-2020, 2020-2021, and 2021-2022.

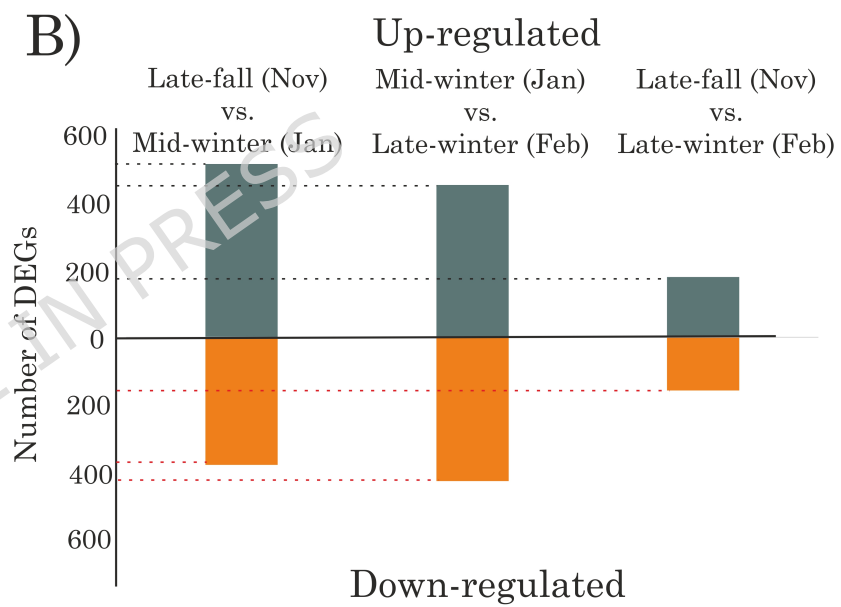
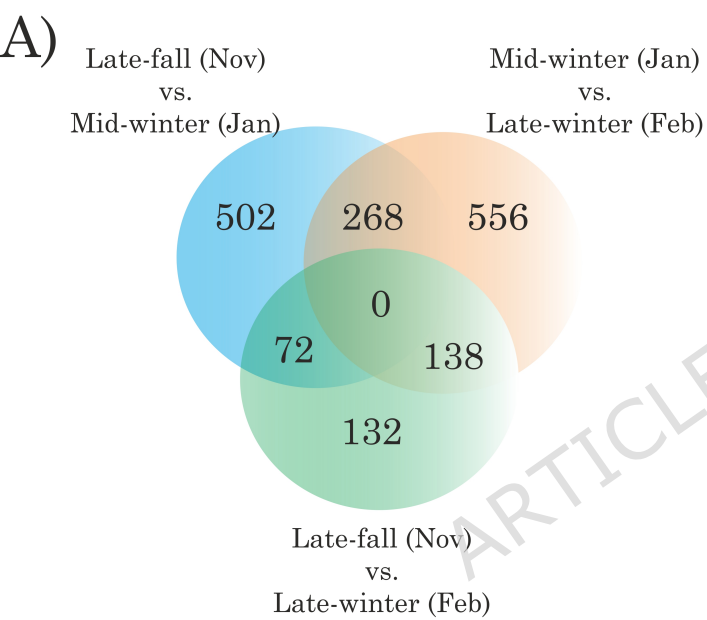
	ANOVA					Tukey Test		
	Sum of squares	df	Mean squares	"F"	"p"	Comparison	Tukey's Q-values	"p"
Between groups	8470.32	3	2823.44	434.7	4.74E-225	Nov. vs. Dec.	30.37	0
Within groups	15412.3	237	6.49486			Nov. vs. Jan.	29.81	0
Total	23882.6	237	1.00E-05			Nov. vs. Feb.	4.366	0.0
		6				Dec. vs. Jan.	0.8809	2
						Dec. vs. Feb.	39.89	0

Jan. vs.		
Feb.	39.02	0

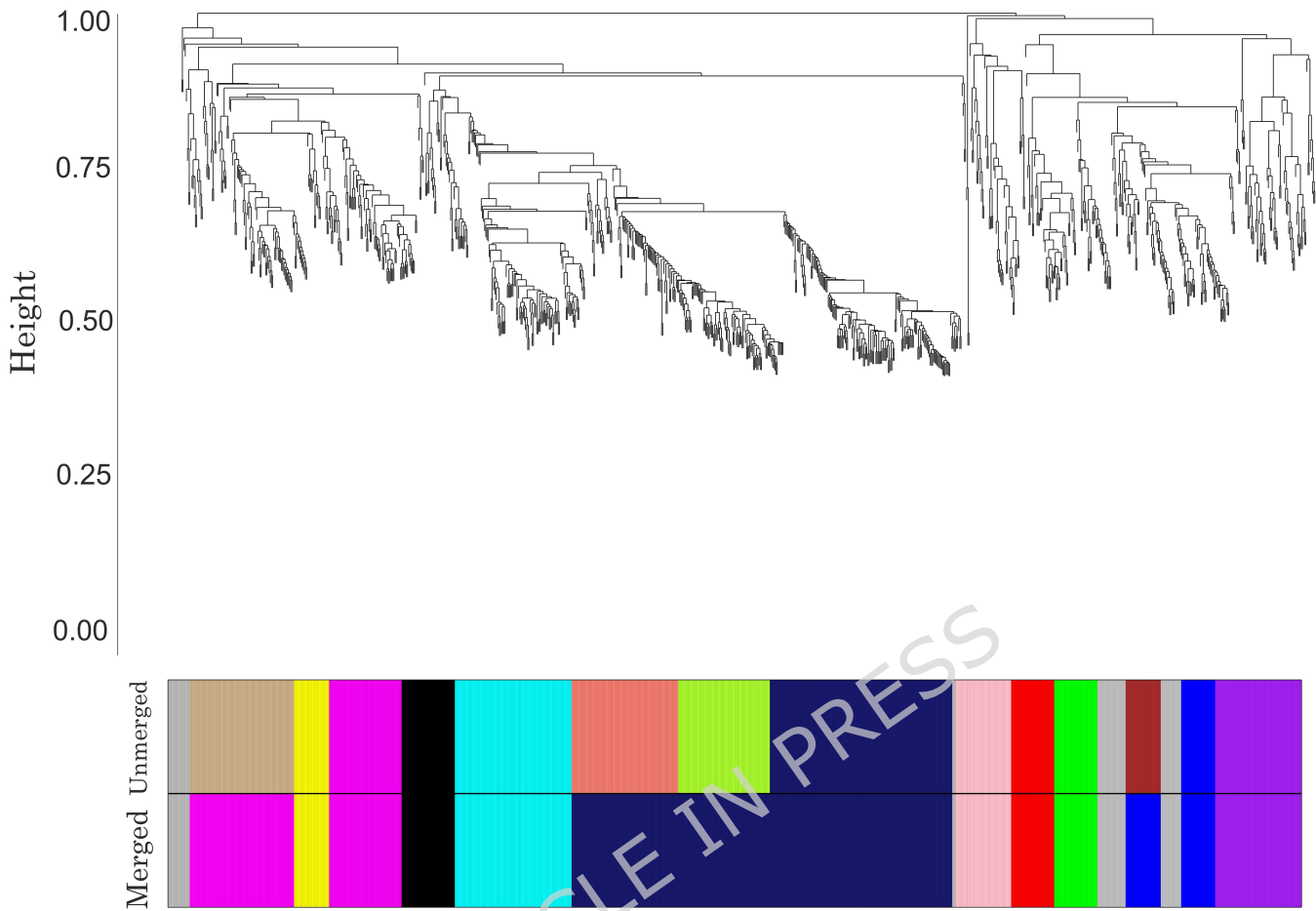
---

The number of temperature records in the stem and in the hibernaculum by month were 6,480. The total number of temperatures records per microsite (stem and hibernaculum) were 25,920 and the total data set of temperature records were  $n = 51,840$  temperature records. **Note: Tukey's test is showed in the table S2.**

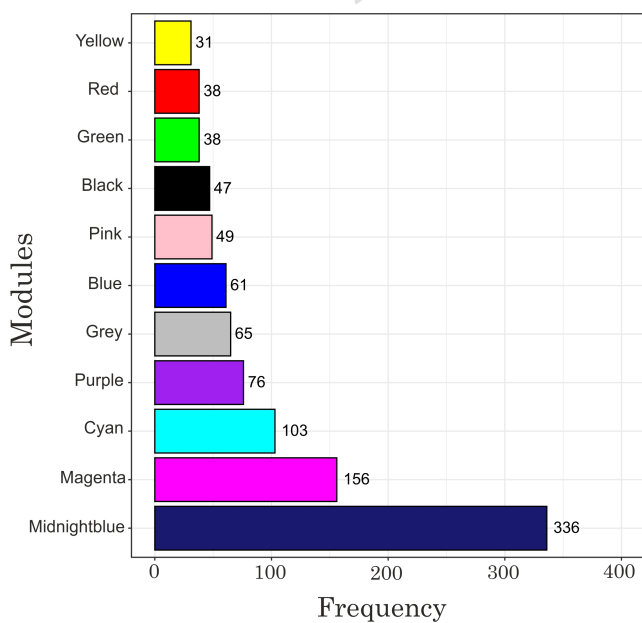
ARTICLE IN PRESS



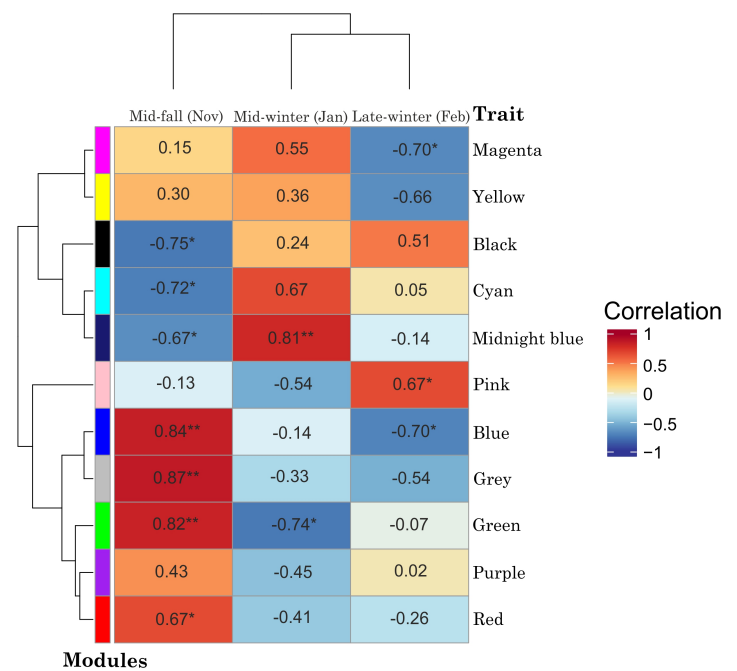
A) Dendrogram of genes and modules



B) Number of genes per module

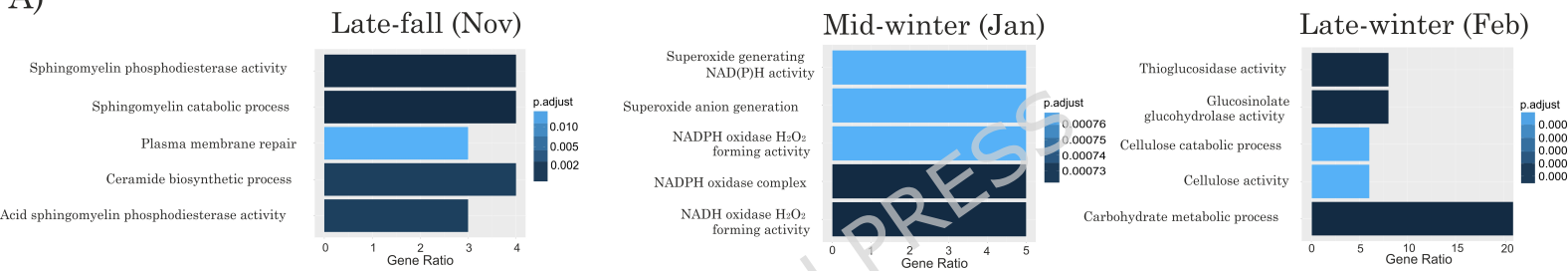


C) Module-trait correlation



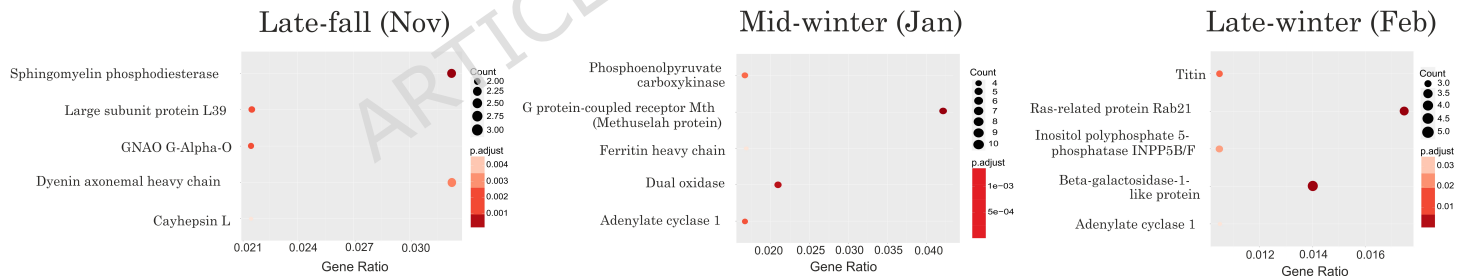
## GO Enrichment

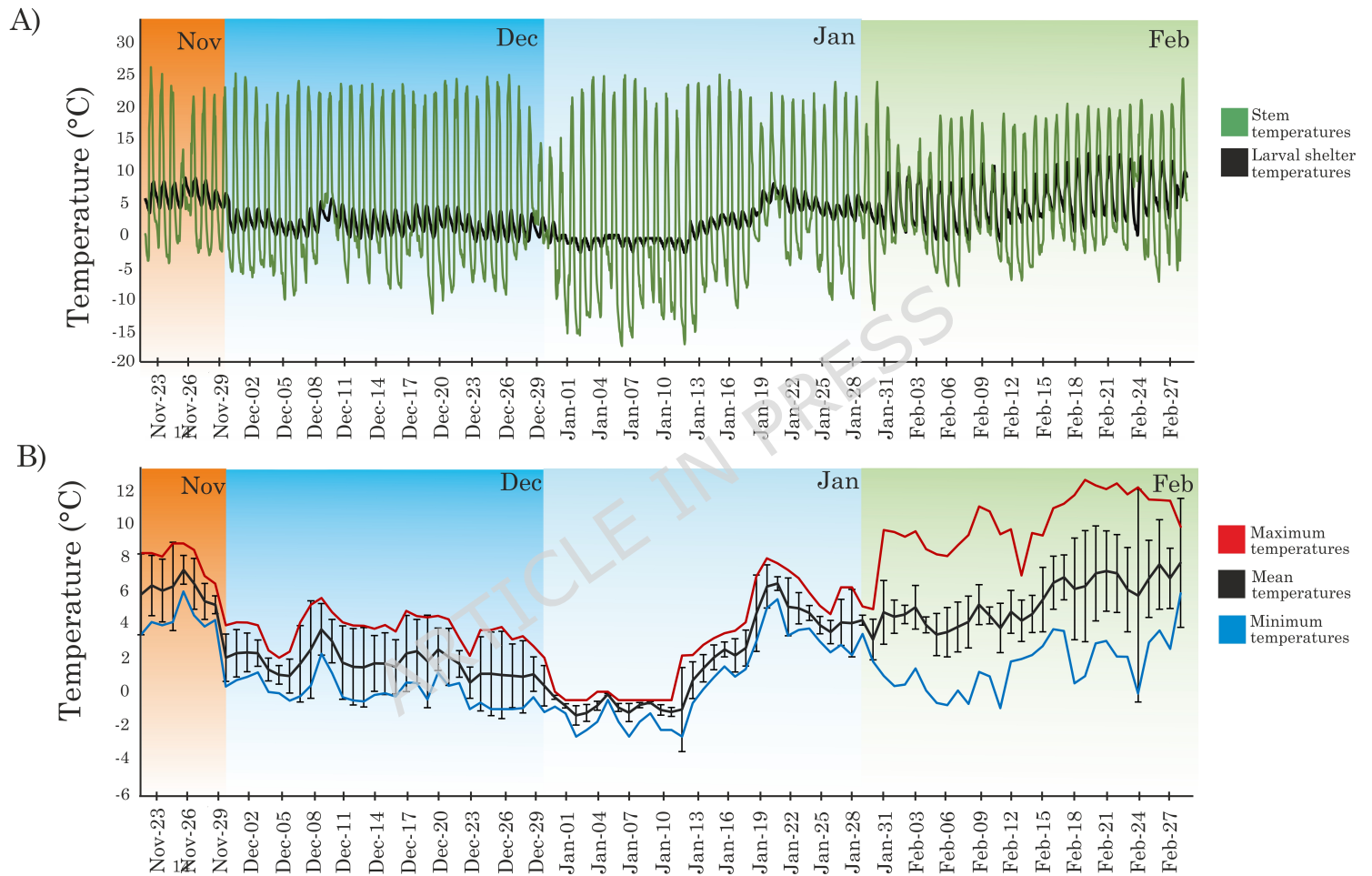
A)



## KEGG Enrichment

B)





Fifth instar larvae

Late-fall

Mid-winter

Late-winter

Blue Module

Grey Module

Green Module

Red Module

Midnightblue Module

Pink Module

Biological process

Molecular function

Cellular component

- Cellulose catabolic process
- Digestion
- Proteoglycan metabolic process
- Positive regulation of endothelial growth factor
- Heparanate sulfate proteoglycan catabolic process
- Fructose 1,6-bisphosphate metabolic process
- Glycosidase catabolic process
- Angiogenesis involved in wound healing
- Fructose metabolic process
- Carbohydrate metabolic process
- Cytoplasmic translation
- Proteolysis involved in cellular protein catabolic process
- Translation
- Proteasomal ubiquitin-independent protein catabolic process
- Cellular iron ion homeostasis
- ATP synthesis coupled proton transport
- Iron ion transport
- Chaperone-mediated protein folding
- Regulation of myoblast fusion
- Endosome transport via multivesicular body sorting pathway
- mRNA splicing, via spliceosome
- Formation of cytoplasmic translation initiation complex
- Cell wall modification
- Pectin catabolic process
- ether lipid biosynthetic process
- Cellulase activity
- Methyl indole-3-acetate sterase activity
- Beta galactosidase activity
- Hexanase activity
- Syndecan binding
- Beta-glucuronidase activity
- Cellulase 1,4-beta-cellobiosidase activity
- (1->8;3)-beta-D-glucan binding
- 6-phosphofructo-2-kinase activity
- Fructose-2,6-bisphosphate 2-phosphatase activity
- Serine-type carboxypeptidase activity
- Hydrolase activity, acting on ester bonds
- Polysaccharide binding
- Metalloprotease activity
- Hydrolase activity, hydrolyzing O-glycosyl compounds
- Juvenile-hormone esterase activity
- Cysteine-type peptidase activity
- Structural constituent of ribosome
- Odorant binding
- Acid phosphatase activity
- Cysteine-type endopeptidase activity
- Collagen binding
- NAD binding
- Serine-type peptidase activity
- Translation initiation factor activity
- Ferroxidase activity
- Proton-transporting ATP synthase activity, rotational mechanism
- Proton transmembrane transporter activity
- Unfolded protein binding
- Endopeptidase activity
- NADH dehydrogenase (ubiquinone) activity
- Thioglycosidase activity
- Glucosinolate glucohydrolase activity
- Hydrolase activity hydrolyzing O-glycosyl compounds
- Cellulose 1,4-beta-cellobiosidase activity
- Pectinesterase activity
- Aspartyl esterase activity
- D-threo-aldose 1-dehydrogenase activity
- Specific granule lumen
- Vacuole
- Lysosomal lumen
- Cytosolic ribosome
- Ribosome
- Proteasome core complex
- Proteasome complex
- Mitochondrial proton-transporting ATP synthase complex
- Proteasome core complex, alpha-subunit complex
- Eukaryotic 43S preinitiation complex
- Small ribosomal subunit
- Proton-transporting ATP synthase complex, catalytic core F(1)
- Mitochondrial respiratory chain complex I
- Catalytic step 2 spliceosome
- Precatalytic spliceosome
- Melanosome

Table 1. ANOVA and Tukey's post hoc test of mean temperatures recorded in the hiberna

<b>ANOVA</b>						
	Sum of squares	df	Mean squares	"F"	"p"	Comparisson
Between groups	8470.32	3	2823.44	434.7	4.74E-225	Nov. vs. Dec.
Within groups	15412.3	2373	6.49486			Nov. vs. Jan.
Total	23882.6	2376	1.00E-05			Nov. vs. Feb. Dec. vs. Jan. Dec. vs. Feb. Jan. vs. Feb.

The number of temperature records in the stem and in the roots by month were 6,480. Tr

riculum from November to February of the years 2019-2020, 2020-2021, and 2021-2022.

<b>Tukey Test</b>	
Tukey's Q-value:	"p"
30.37	0
29.81	0
4.366	0.01
0.8809	0.92
39.89	0
39.02	0

The total number of temperatures records per microsite (stem and root) were 25,920 and tr

the total data set of temperature records were  $n = 51,840$  temperature records. Note: Tuke

ARTICLE IN PRESS